



Covalent organic framework membranes for selective ion separation



Fangmeng Sheng, Liang Ge , Xingya Li & Tongwen Xu

Ion-selective membranes play a crucial role in addressing water scarcity, environmental security, and energy utilization. Conventional microphase separation membranes suffer from trade-off limitation between permeability and selectivity due to the poor dimensional stability of ion-conductive regions. Microporous membranes utilize rigid polymer backbones to mitigate the trade-off effect, yet their tortuous pore connections hinder efficient ion separation. Covalent organic frameworks (COFs), known for their regular pore structures with permanent porosity and facilely tailored functionality, are anticipated as new-generation membrane materials. In this review, we elaborate on the potential and challenges of COF membranes from structural design, preparation protocols, and separation applications. Furthermore, we propose future opportunities and research trends for COF membranes, particularly in the scale-up fabrication, demanding ion separation system and genuine selective ion transport mechanism.

Ion-selective transport processes play a pivotal role in diverse fields, including desalination, chemical separation, environmental protection, energy storage and conversion, and life sciences^{1–4}. For instance, desalination relies on the selective removal of salt ions, while chemical separation processed, such as lithium and rare-earth metal extraction, require precise transport of target ions. In energy systems (e.g., osmotic energy harvesting, flow batteries), efficient and selective ion transport is critical for device performance. Biological systems, notably cell membranes, achieve ion-specific transport through channel proteins to sustain life activities. Thus, understanding and controlling selective ion transport holds profound implications across energy, environment, and life science domains.

Ion-selective membranes, serving as efficient media for regulating ion transport and separation, have undergone rapid development owing to their high separation efficiency, low energy consumption, ease of system integration, and environmental friendliness^{4–6}. In recent years, the accelerated advancement of new energy technologies has boosted surging demand for high-performance ion-selective membranes in critical applications such as lithium extraction from salt lakes, rare-earth metal ions recovery, and electrochemistry systems^{7–10}. Concurrently, these emerging applications impose enhanced requirements on new-generation ion-selective membranes, particularly in terms of high transport efficiency, precise separation capability, chemical stability, and scalable manufacturing. Conventional polymer materials have been widely used to prepared ion-selective membrane across all scales in practical applications, benefiting from their low cost and scalability. The representative membranes are perfluorocarbon Nafion and hydrocarbon-based polyelectrolytes, which are prepared by self-

assembly to form ion conductive regions via microphase separation (Fig. 1a)^{11–13}. However, these regions are ill-defined and exhibit poor dimensional stability in solvents due to swelling, which ruins the ion selectivity, resulting in a well-known trade-off between ion permeability and selectivity and constraining the advancement of ion-selective membranes in high-efficient precise ion separation.

In recent years, advanced porous membranes featuring nano-/sub-nanochannels have become the focus in ion separation due to their high porosity, continuous transport pathways, low resistance, and tunable channel surface properties^{2,14}. These characteristics enable such membranes to overcome the permeability-selectivity trade-off typical of conventional polymer membranes. For instance, porous polymer membranes create pores by modulating polymer chain packing or branched chain crosslinking, including hypercrosslinked polymers (HCPs)¹⁵, polymers of intrinsic microporosity (PIMs)^{16,17}, and conjugated microporous polymers (CMPs)¹⁸. Taking PIMs as an example, the introduction of moderately rigid monomers and their atomic non-planar distortion inhibits chain packing and create inherent micropores (Fig. 1b). Nevertheless, their disordered sub-nanochannels, ill-defined structural parameters, and presence of dead-end pores increase ion transport resistance and complicate mechanistic studies under confined space. Moreover, non-network PIMs also suffer from aging and swelling-induced loss of selectivity under high charge density conditions. Two-dimensional (2D) materials, including graphene, graphene oxide (GO), molybdenum disulfide (MoS₂), hexagonal boron nitride (hBN), transition-metal carbides and nitrides (MXene), and layered double hydroxides (LDHs), enable the construction of channels with atomic

Department of Applied Chemistry, School of Chemistry and Materials Science, University of Science and Technology of China, Hefei, PR China.

e-mail: xingyali@ustc.edu.cn; twxu@ustc.edu.cn

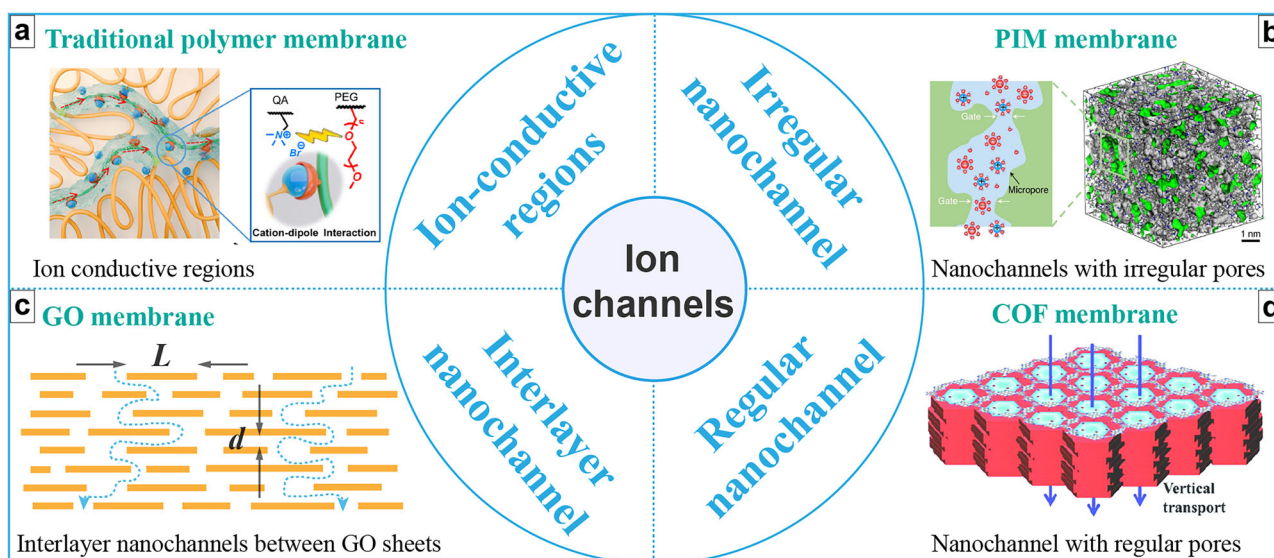


Fig. 1 | Ion-selective channels in various membranes. **a** Conventional polymer membranes form ion-conductive regions through microphase separation self-assembly between hydrophobic and hydrophilic domains. Reproduced with permission from ref. 13. (copyright Wiley-VCH, 2021). **b** Microporous membranes represented by polymers of intrinsic microporosity (PIMs) with irregular sub-nanochannels through non-planar polymer chain packing. Reproduced with

permission from ref. 16. (copyright Springer Nature, 2020). **c** 2D membranes exemplified by GO with tortuous interlayer nanochannels via nanosheets assembly. Reproduced with permission from ref. 20. (copyright American Association for the Advancement of Science, 2012). **d** 2D COF membranes with intrinsic 1D regular nanochannels of permanent porosity and precisely tunable functionalities. Reproduced with permission from ref. 25. (copyright Royal Society of Chemistry, 2018).

precision via nanosheet assembly^{14,19}. However, their in-plane non-productive pathways elongate ion transport routes²⁰. For example, a 1 μm -thick GO membrane assembled by 500 nm nanosheets can exhibit an ion transport path of $\sim 1\text{ mm}$ —1000 times of its thickness (Fig. 1c). In comparison, crystalline porous framework materials, such as metal-organic frameworks (MOFs) and covalent organic frameworks (COFs), offer inherent advantages for constructing high-efficiency ion-selective channels due to their pre-designable crystalline frameworks, ordered pore structures, and high porosity²¹. Among them, COFs exhibit superior chemical stability, rendering them more viable for precision ion separation applications^{21–24}. In particular, 2D COFs with vertically aligned one-dimensional (1D) channels enable the minimal pathways and stable ion flow, promising to achieve unprecedented ion transport efficiency and break the permeability-selectivity trade-off (Fig. 1d)²⁵.

COFs represent a novel class of crystalline organic porous materials comprising of periodically extended and covalently bounded network structures. They exhibit well-defined pore structures with atomic precision, permanent porosity, facile functionalization, and exceptional hydrolytic stability, making them highly attractive for membrane separation applications^{24–30}. Recently, COF membranes have garnered increasing interest for molecular and ionic separations, especially in Ångström-scale precision separations^{22–24}. This review systematically summarizes recent advances in COF membranes, covering structural design, fabrication strategies, and ion separation applications, while also addressing current challenges and future directions. Special emphasis is placed on crystallization-controlled membrane formation mechanism, green fabrication and evaluation of large-area COF membranes, bioinspired ion transport mechanisms, and AI-assisted computational screening and structural design.

Structural design of COFs

Skeleton structure

In 2005, Yaghi et al. pioneered COFs synthesis via boroxine (COF-1) and boronate ester (COF-5) linkages²⁷, marking the first construction of crystalline porous organic frameworks. Since then, various reversible reactions have been employed to synthesize COFs, which can be classified into non-conjugated, partially conjugated, and fully conjugated skeletons based on their linkage chemistry (Table 1)^{29,31}. Non-conjugated COFs typically

Table 1 | COFs with different skeletons constructed via various organic reactions

Non-conjugated skeleton	Partially conjugated skeleton	Fully conjugated skeleton
Boroxine linkage	Imine linkage	β -ketoenamine linkage
Boronate ester linkage	Azine linkage	Phenazine linkage
Imide linkage	Hydrazone linkage	C = C linkage
Amide linkage	Triazine linkage	
Dioxin linkage	Benzoxazole linkage	
Borazine linkage	Squaraine linkage	
Spiroborate linkage	Azodioxy linkage	
Borosilicate linkage	Viologen linkage	

incorporate linkages such as boroxine²⁷, boronate ester^{27,32}, imide^{33,34}, amide³⁵, dioxin³⁶, borazine³⁷, spiroborate³⁸, and borosilicate³⁹. Partially conjugated COFs have been designed using imine^{40–42}, azine^{43,44}, hydrozone⁴⁵, triazine^{46,47}, benzoxazole⁴⁸, squaraine⁴⁹, azodioxy⁵⁰, and viologen⁵¹ linkages. Fully conjugated COFs include β -ketoenamine^{52–55}, phenazine⁵⁶, and C=C linkages^{57,58}. These diverse linkages endow COFs with exceptional potential for adsorption, separation, catalysis, and energy storage. Although a considerable number of COF linked skeleton structures developed, only a few of these structures have been prepared into membranes, given considerations such as their stability and synthesis conditions. Currently, the most widely reported COF skeletons for ion separation are based on imine linkages formed via Schiff-base reactions, owing to their favorable crystallization under mild conditions and robust framework stability. For example, Dey et al.⁵⁹ developed an interfacial crystallization strategy to prepare a series of imine-linked COF membranes under ambient conditions. Owing to the abundant electronegative C=N bonds in imine-linked COF skeletons, they exhibit a distinct responsiveness to environmental pH. For instance, Cao et al.⁶⁰ further introduced phenolic hydroxyl groups into the monomers, synthesizing an oriented COF-DT membrane with high ion flux and stimuli-responsive behavior, enabling precise modulation of ion transport through pH-triggered changes in both imine and

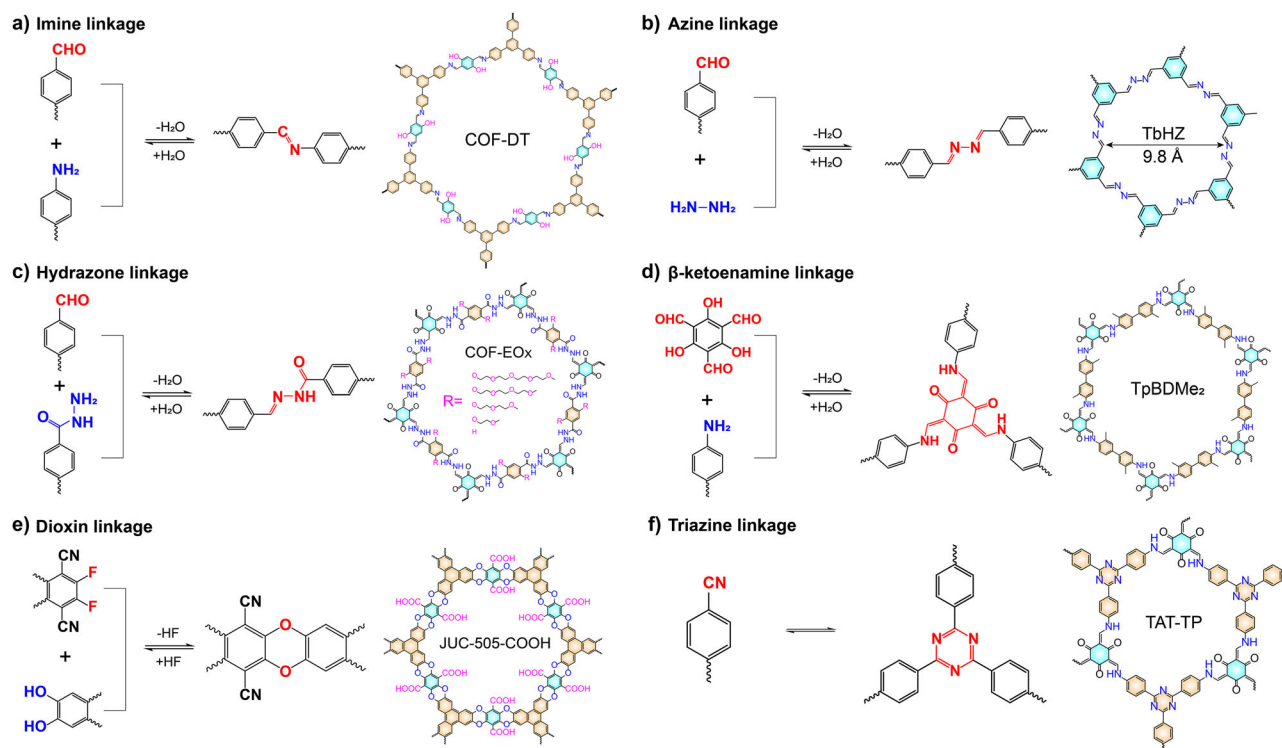


Fig. 2 | Different types of linkages of COF skeletons for ion separation. (a) Imine linkage COF skeleton and the representative COF-DT for ion separation⁶⁰. (b) Hydrazine hydrate was applied to construct azine linkage COF skeleton and the representative TbHZ with subnanochannels for ion separation⁶¹. (c) The hydrazide monomers were utilized to synthesize hydrazone linkage COF skeleton and the

representative COF-EOx for ion separation⁶². (d) Tp monomer was used to synthesize β-ketoenamine linkage COF skeleton and the representative TpBDMe₂ for ion separation⁶³. (e) Dioxin linkage COF skeleton and the representative JUC-505-COOH for ion separation⁶⁵. (f) Triazine linkage COF skeleton and the representative TAT-TP for ion separation⁶⁶.

phenolic moieties (Fig. 2a). Beyond conventional imine linkages, azine-linked COFs can be synthesized using hydrazine hydrate and aldehyde monomers. The small molecular size of hydrazine hydrate (HZ) enables the construction of COF membranes with sub-nanometer pores. Yin et al.⁶¹ prepared a hydrazone-linked TbHZ membrane with vertically aligned sub-nanometer channels, exhibiting high precision ion separation for ions differing in size at 2 Å (Fig. 2b). In addition, the reaction between hydrazide monomers and aldehyde monomers was utilized to synthesize COFs with hydrazone linkages. Meng et al.⁶² reported a series of hydrazone-linked COF membranes with different lengths of the oligoether segments, systematically regulating pore solvation environments and elucidating how solvating segments influence ion partitioning, diffusion, and selectivity (Fig. 2c). To enhance the chemical stability of COFs under harsh acidic or basic conditions, Kandambeth et al.⁵² introduced the 1,3,5-triformylphloroglucinol (Tp) monomer, which first forms an imine-linked framework via a reversible Schiff-base reaction, followed by an irreversible enol–keto tautomerization to yield a more stable β-ketoenamine-linked structure while maintaining a crystallinity. This advancement significantly broadened the application scope of COFs. In our group, we constructed a 20 nm ultrathin β-ketoenamine-linked COF membrane on an anodic aluminum oxide (AAO) substrate and demonstrated that abundant hydrogen bonding sites in the channels can form hydrogen bonding interaction with water (Fig. 2d)⁶³. We reveal that the hydrogen bonding interaction between hydrated cations and channel walls govern the ion selectivity, with divalent cations experiencing higher energy barriers for transport compared to monovalent ions. We also developed freestanding β-ketoenamine-linked COF membranes and demonstrated their utility in acid and alkali recovery⁶⁴. In addition, Zhu et al.⁶⁵ prepared a dioxin linkage oxygen-rich COF and showed its potential in efficient removal of Cd(II) and Pb(II) from water (Fig. 2e). Since the direct synthesis of triazine-linked COFs typically requires harsh conditions, Meng et al.⁶⁶ developed an alternative strategy by reacting a triazine-functionalized amine monomer with Tp under mild

conditions (Fig. 2f). This approach yielded a triazine-linked COF membrane capable of high-resolution Li⁺/Mg²⁺ separation. The hydrophilic channel environment promotes Li⁺ dissociation from sulfonate groups, facilitating hopping transport along sulfonate-functionalized side chains and shortening the Li⁺ diffusion path.

Pore engineering

The regular pore structure is one of the most fascinating features of COFs, especially for membrane separation. Atomic-level pore engineering is achievable through four main strategies including topology control, monomer design, synthetic condition, and post-synthetic functionalization^{29–31}. Firstly, monomer geometry and topology dictate COF pore shapes (hexagonal/quadrilateral/triangular)^{46,67–71}, while the chemical structure of monomer enable dual-pore systems with co-existing geometries or dimensionally varied hexagons (Fig. 3a). For example, Meng et al.⁷² utilized benzene-1,3,5-tricarbohydrazide as the core building block to react with aldehydes owing different reaction sites and synthesized 0.78 nm and 1.58 nm COF membranes with similar chemistry by [2 + 3] and [3 + 3] topology configuration. Li et al.⁷³ adjusted the chemical structure of aldehyde monomer to regulate the pore size of COF membranes from >1 nm to sub-1-nm scale by changing the stacking mode of COF layers from AA to AB stacking. Chen et al.⁷¹ introduced PyTTA (4,4',4''-(pyrene-1,3,6,8-tetra-yl) tetraaniline) monomer to synthesize quadrilateral single-pore COF, while Pang et al.⁷⁴ used the similar symmetric amine monomer but different chemical structure and synthesized a dual-pore COF, which possesses both micropores and mesopore. Furthermore, Zhao et al.^{75,76} designed asymmetric monomer to create COFs with tri- and tetra-pore systems.

Apart from topology control, monomer design offers precise control over pore dimensions. While most COFs exhibit pore sizes in the range of 1 ~ 3 nm⁷⁷, judicious monomer elongation allows tuning from the sub-nanometer scale to expanded mesopores. As illustrated in Fig. 3b, monomer elongation can precisely modulate the pore size of COF. Sun et al.⁷⁸ utilized

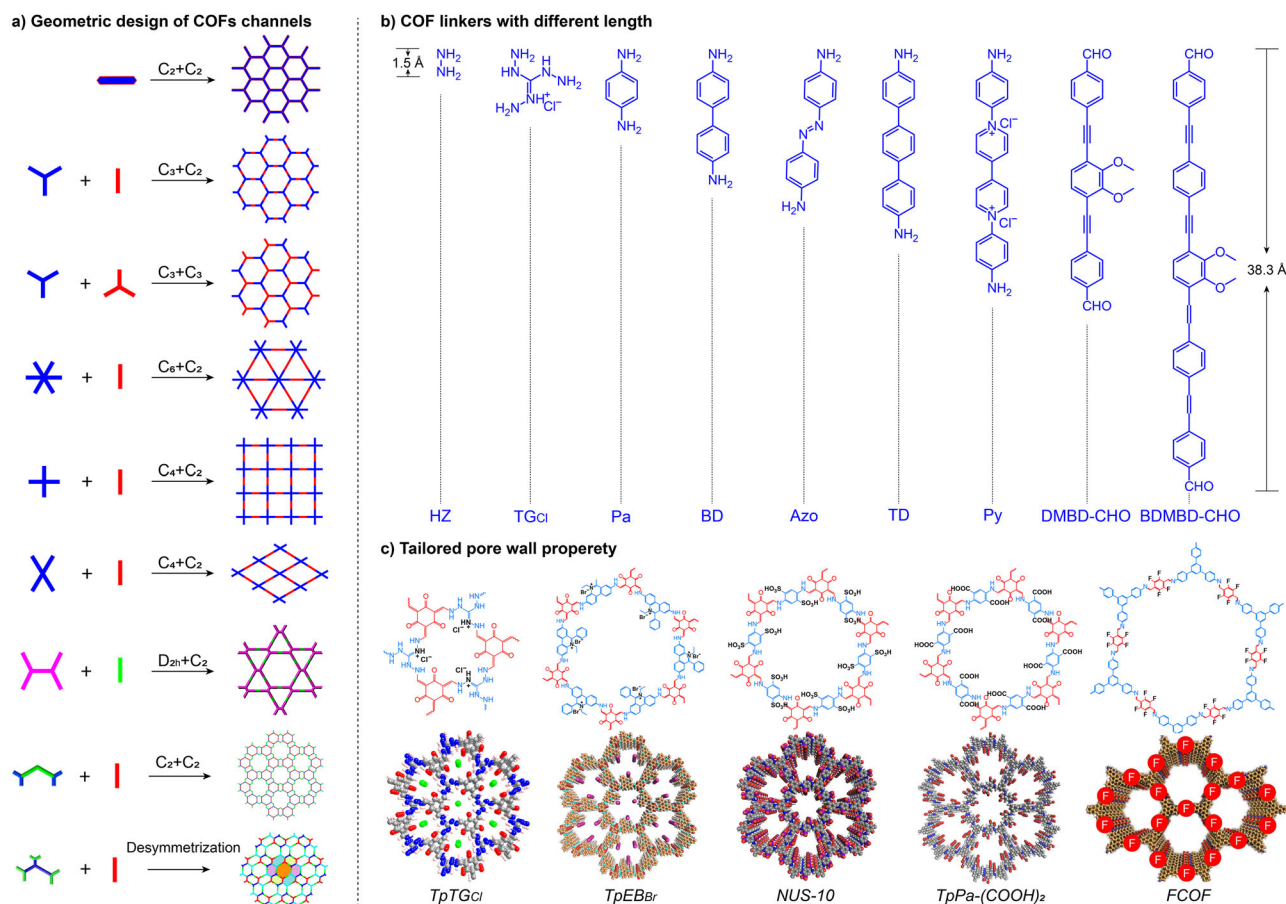


Fig. 3 | Pore engineering of COFs. (a) Pore geometric engineering of COFs through modulating monomer geometries and topological connectivity. Reproduced with permission from refs. 30,74–76. (copyright American Chemical Society, 2016, 2017 and 2019; Springer Nature, 2019). (b) Pore size engineering by designing COF

linkers with different length^{52,68,78,79,94}. (c) Pore chemical engineering by introducing different functional groups into the monomers. Reproduced with permission from refs. 68,81–84. (copyright American Chemical Society, 2016; Springer Nature, 2021).

HZ monomer and synthesized COF membrane with pore size of 0.73 nm, while Mu et al.⁷⁹ employed elongated linear linkers to synthesize mesoporous COFs with pores up to 10 nm. In addition, the channel chemistry of COFs is programmable through functional monomers, yielding positive (cationic/quaternary ammonium salts)^{68,80,81}, negative (sulfonic/carboxylic acids)^{82,83}, hydrophobic (fluorine-containing)⁸⁴, and other functionalized channels (Fig. 3c)⁹⁷. Synthetic condition is another important factor defining COF pore structure. Yin et al.⁶¹ introduced a solvent vapor annealing approach that weakens π - π interactions between COF layers, promoting reorientation from random stacking to a face-on configuration with vertically aligned pores. Similarly, Sun et al.⁷⁸ achieved partial regulation of the pore orientation of COF membranes by using different organic solvent in interfacial polymerization. Post-synthetic functionalization strategy is also widely used to modulate the pore structure of COFs. Meng et al.⁷ incorporated olefin units into COF frameworks and conducted post-functionalization to manipulate the pore charge density by the thiol-ene click reaction. Ren et al.⁸⁵ constructed biomimetic smart COF membranes with charged and switchable sub-nanochannels through grafting photo-responsive azobenzene derivatives onto channel wall via the sulfur(VI) fluoride exchange (SuFEx) click reaction. Our group has also reported negatively and positively charged COF membranes through post-modification with propanesulfonate and iodomethane, respectively⁶⁴. Finally, hybridization with other materials provides an additional route to tailor pore structure of COF membranes. Yang et al.⁸⁶ adapted the sheltering effect of 1D cellulose nanofibers (CNFs) to regulate the pore size of COF membrane (0.45–1.0 nm) through a mixed-dimensional assembly of 2D COF nanosheets and 1D CNFs. Wang et al.⁸⁷ reported a 2D COF membrane

with narrowed channels (0.7 nm \times 0.4 nm) and excellent mechanical performance constructed by the staggered stacking of cationic and anionic 2D COF nanosheets.

Preparation of COF membranes

Although Yaghi et al.²⁷ pioneered the synthesis of 2D COFs (i.e., COF-1 and COF-5) in 2005 and developed 3D COFs two years later⁸⁸, the poor solution processability of COFs delayed their membrane applications. It was not until 2011 that the first COF-5 membrane supported on single-layer graphene was prepared via an in situ growth method³², marking the beginning of COF membrane research (Fig. 4). Subsequently, advances in COF nanosheet exfoliation enabled membrane fabrication through nanosheet assembly^{89–92}. Furthermore, polymer blending with COFs emerged as an effective approach for producing COF-based mixed matrix membranes (MMMs)⁹³. A notable acceleration occurred in 2017 through two studies by Banerjee et al., which prepared pure-phase COF membranes via interfacial polymerization⁵⁹ and casting dough⁹⁴ methods, respectively. Meanwhile, more advanced methods such as electrophoretic deposition (EPD)^{95,96}, chemical vapor deposition (CVD)⁹⁷, Langmuir-Blodgett (LB) assembly⁹⁸, compression⁹⁹, and phase switching¹⁰⁰ have been successfully implemented, significantly expanding their potential applications.

Conventional preparation methods

In the early stages, due to the poor solution processability of COF materials and the harsh synthesis conditions, in situ growth was employed for the fabrication of COF membranes. In 2011, Colson et al.³² demonstrated this approach by synthesizing COF-5 membrane on single-layer graphene

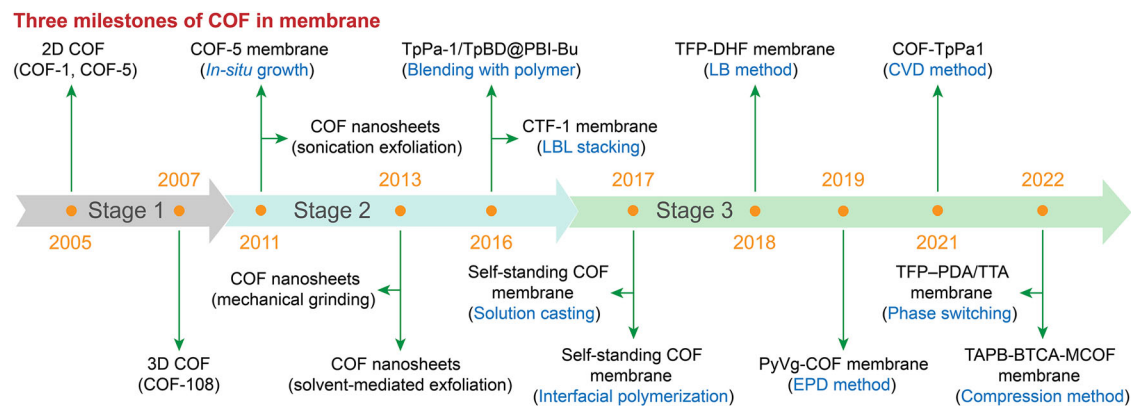


Fig. 4 | The evolution history of COF membranes. Three milestones throughout the development of COF membranes^{27,32,54,59,88–91,93–95,97–100}

substrates. This methodology was subsequently adapted to diverse substrates: Yang et al.¹⁰¹ (2012) and Hao et al.¹⁰² (2014) extended the synthesis of COF-5 membrane on alumina disks and APTES-modified α -Al₂O₃ substrates, respectively. In addition, Fu et al.¹⁰³ prepared a [COF-300]-[ZIF-8] composite membrane on polyaniline coated SiO₂ disk via in situ growth in 2016. Further developments were achieved in 2018 by Fan et al.¹⁰⁴, who synthesized imine-based COF-LZU1 membranes on Al₂O₃ tubes. The same year, they prepared COF-LZU1 – ACOF-1 bilayer membranes on APTES-Al₂O₃ substrate¹⁰⁴. Recent advancements include Wu et al.¹⁰⁵ (2025) using in situ growth to prepared imine-based 3D COF membranes with highly charged sub-nanochannels on APTES-modified DPAN substrates and achieving remarkable lithium-ion sieving capabilities. Although in situ growth represents a pioneering and important methods for synthesizing COF membranes—enabling precise modulation of crystallinity and orientation through substrate surface engineering—this method faces several critical limitations. Firstly, the method typically requires harsh synthesis conditions, including prolonged reaction time at elevated temperatures under sealed environments, high material consumption, and low membrane-yield efficiency, which inevitably increase the challenge of scalability. Furthermore, the abundant consumption of organic solvents and rigorous selection of substrate in terms of chemical stability and surface properties restricts the development of this method to some extent, especially for large-scale membrane production. Meanwhile, the advancement of exfoliation techniques for 2D COFs has stimulated substantial research efforts in COF nanosheet fabrication^{54,89,90,92}. Inspired by GO membrane, layer-by-layer (LBL) assembly has evolved as a robust method for COF membrane preparation. In 2016, Ying et al.⁹¹ reported the first fabrication of a 2D covalent triazine-based framework-1 (CTF-1) membrane on a cellulose acetate support with GO assistance via the LBL strategy. In 2020, the author further prepared TpEBr@TpPa-SO₃Na hybrid membranes on porous α -Al₂O₃ support by LBL assembly of oppositely charged ionic COF nanosheets with distinct pore sizes¹⁰⁶. Li et al.¹⁰⁷ prepared boroxine linkage COF-1 membrane by assembling COF-1 nanosheets on ceramic substrates. Jiang et al.⁸⁶ developed mixed-dimensional TpTG_{Cl}@CNFs membranes by assembling 1D CNFs and 2D TpTG_{Cl} nanosheets on PAN substrates, enabling precise molecular sieving and desalination. Subsequently, they synthesized ionic COF nanosheets via oil–water–oil triphase synthesis and assembled DhaTG_{Cl}/PAN membranes¹⁰⁸. Then, they further utilized adhesion-engineering to assemble TpPa-SO₃H@TpTTPA membranes via electrostatic and π - π interactions, achieving exceptional NaCl rejection (99.91%) and high salinity (7.5 wt%) tolerance¹⁰⁹. The LBL assembly has emerged as a versatile platform for preparing 2D material membranes, offering atomic-level precision in regulating membrane thickness, interlayer spacing, and channel properties. In addition, the assembly procedure is very easy and high efficiency. However, the synthesis of COF nanosheets is time-consuming and the membrane performance remains fundamentally constrained by the structural uniformity of 2D nanosheets (particularly monodispersity and defect density), while the dispersion of nanosheets also

require abundant consumption of organic solvents. In addition, the long-term structural integrity of assembled membranes persists as a critical limitation, which confronts inherent scalability barriers in industrial implementation, particularly for roll-to-roll or continuous manufacturing paradigms. Blending COF bulk powders or nanosheets with polymers represents a straightforward methodology for preparing COF-based MMMs. For instance, Biswal et al.⁹³ combined COF powders with polybenzimidazole (PBI) at varied mass ratios to prepare freestanding COF@PBI-BuI-based MMMs. Mitra et al.⁶⁸ synthesized self-exfoliated guanidinium-based ionic COF nanosheets and blended them with polysulfone (PSF) to fabricate TpTG_{Cl}@PSF MMMs. Similarly, Peng et al.⁸² incorporated negatively charged COF powders (NUS-9 and NUS-10) into nonconductive polyvinylidene fluoride (PVDF), achieving COF@PVDF MMMs with high proton conductivity. COF-based MMMs prepared through polymer blending exhibit exceptional simplicity, high efficiency, and scalability. However, such membranes frequently suffer from interfacial gaps between COF fillers, poor polymer-COF compatibility, and non-uniform spatial distribution of COF particles coupled with stochastic orientation of COF nanochannels within the polymer matrix—critical limitations that fundamentally constrain their inherent separation capabilities.

Emerging preparation methods

A significant acceleration in COF membrane occurred in 2017, marked by the introduction of interfacial polymerization as a representative strategy. Banerjee et al.⁵⁹ pioneered the synthesis of freestanding imine-linked COF membranes via interfacial polymerization at water/organic interfaces. Shortly after, Valentino et al.¹¹⁰ prepared polyimine COF TFC nanofiltration membrane on polyethersulfone (PES) substrates through interfacial polymerization. Since then, the preparation of COF membranes through interface polymerization has attracted extensive research interest. In recent years, advancements in interfacial polymerization have enabled the development of diverse reaction systems across liquid-liquid^{29,111}, aqueous-aqueous¹¹², solid-vapor¹¹³, liquid-vapor¹¹⁴, and liquid-solid¹¹⁵ interfaces. Matsumoto et al.¹¹¹ prepared freestanding TAPB-PDA COF membranes by layering a dioxane/mesitylene organic phase (dissolving aldehyde and amine monomers) over an aqueous phase containing Sc(OTf)₃ Lewis acid catalyst. Li et al.⁷³ engineered DCM/DMF organic-organic interfaces to construct AA- and AB-stacked COF membranes, where AB-stacked membranes with ordered nanosheets exhibited sub-nanometer pores (~0.6 nm). Wang et al.¹¹² established a dextran/poly(ethylene glycol) aqueous two-phase system (ATPS) to construct freestanding COF membranes, revealing that interfacial tension has pronounced effect on membrane structures. Innovative strategies have further expanded fabrication precision. Sheng et al.⁶³ synthesized ultrathin COF membranes (~20 nm) on AAO via a counter-diffusion strategy. Khan et al.¹¹³ achieved solid-vapor interfacial polymerization by vaporizing p-phenylenediamine (PDA) and octanoic acid (OA) onto APTES-modified Si/SiO₂ disk loading with 1,3,5-Triformylphloroglucinol (TFP) monomer, forming TFP-PDA membrane.

Table 2 | Comparison of methods for COF membranes synthesis based on procedure, efficiency, quality, scalability, sustainability characteristics

Methods	Procedure	Efficiency	Quality	Scalability	Sustainability
In situ growth	Harsh synthesis conditions	Inefficient membrane formation	High crystallinity and orientation, depending on the substrate	Moderate	Abundant organic solvents consumption
LBL assembly	Easy assembly, but time-consuming synthesis for COF nanosheets	High efficiency	High crystallinity, depending on the quality of nanosheets	Moderate	Abundant organic solvents consumption
Blending with polymer	Very easy	High efficiency	Moderate, poor orientation	Excellent scalability	Low organic solvents consumption
Interfacial polymerization	Easy operation, but time-consuming	Inefficient membrane formation	High crystallinity and uniformity	Limited area and complex transfer processes	Abundant organic solvents consumption
Casting dough	Very easy	High efficiency	Moderate, poor orientation	Excellent scalability	Low organic solvents consumption
Electrophoretic deposition	Complex operation	High efficiency	High crystallinity and uniformity	Limited area	Low organic solvents consumption
Chemical vapor deposition	Complex operation	Inefficient membrane formation	High crystallinity and uniformity	Limited area	Low organic solvents consumption
Langmuir-Blodgett	Complex operation	Inefficient membrane formation	High crystallinity and uniformity	Limited area	Abundant organic solvents consumption

Zhang et al.¹¹⁴ designed a sandwich-structured liquid-vapor system using hot ethanol solution containing hydrazine hydrate and mesitylene solution dissolving aldehyde and Sc(OTf)₃ to prepare COF membrane on PAN/AAO substrates. Furthermore, Sahabudeen et al.¹¹⁶ developed a surfactant-monolayer-assisted interfacial synthesis (SMAIS) to prepared large-area, highly crystalline COF membranes at water-air interface. Yang et al.¹¹⁷ utilized diethylenetriamine as a sacrificial go-between to prepare a highly strong, tough, and elastic single-crystal 2D COF membrane at water-air interface via the sacrificial go-between guided synthesis method. In addition, Zhao et al.¹¹⁵ exploited liquid-solid interface to prepare freestanding COF membrane on the wall of glass bottle by layering an aqueous solution of Sc(CF₃SO₃)₃ catalyst with a ethyl acetate solution dissolving aldehyde and amine monomers. Interfacial polymerization has emerged as a pivotal strategy for the precision engineering of COF membranes, with significant progress achieved in developing diverse interfacial reaction systems and optimized polymerization protocols. It exhibits several advantages, such as operational simplicity, high versatility, and the prepared membranes with excellent crystallinity and uniformity. However, COF crystallization necessitates meticulous interfacial stabilization and extended reaction periods (typically several days) to balance reaction-diffusion kinetics and thermodynamic equilibrium at constrained interfaces. Moreover, most interfacial polymerization systems predominantly rely on organic solvents for monomer dissolution, incurring substantial environmental risks and cost inefficiencies. These inherent requirements pose significant challenges for large-scale production and practical implementation of COF membranes. Also in 2017, Banerjee et al.⁹⁴ developed a simple “casting dough” method as an alternative to prepare freestanding COF membranes. Subsequently, they further utilized this method to prepared ultrastable imine-based freestanding COF membranes for sulfuric acid recovery¹¹⁸, highly flexible p-toluene sulfonic acid loaded freestanding COF membranes with superprotonic conductivity ($7.8 \times 10^{-2} \text{ S cm}^{-1}$)¹¹⁹, and a redox active free-standing COF membranes as high-performance supercapacitors¹²⁰. Though the casting dough method offers operational simplicity, high efficiency, and scalability, which have potential for scale-up manufacturing and application. However, the current process suffers from lengthy reaction time and poor controllability, especially the mechanism of membrane formation is unclear. Additionally, the heterogeneous reaction system inherently compromises membrane microstructural densification.

Apart from the aforementioned methods, there are also some other methods used to prepare COF membranes. For instance, Shinde et al.⁹⁸ employed the Langmuir-Blodgett (LB) method to prepare ultrathin COF membrane with four-unit cells thick, achieving precise thickness control via multilayer coating. In 2019, Wang et al.⁹⁵ prepared thickness-tunable cationic COF membranes on electrode surfaces using electrophoretic deposition (EPD). Moreover, Wang et al.⁹⁶ further advanced this technique by rapidly depositing TpPa-SO₃H nanosheets onto AAO substrates via two-cell EPD to create ultrathin anionic COF membranes. In 2021, Hao et al.⁹⁷ utilized chemical vapor deposition (CVD) to synthesize COF-TpPa1 membranes on modified PVDF substrates. In 2022, Martín-Illán et al.⁹⁹ developed freestanding imine-linked COF membranes with superior mechanical properties through compression method. The same year, Khan et al.¹⁰⁰ introduced a phase switching strategy to prepare freestanding COF membranes. As shown in Table 2, an analysis based on five criteria (i.e., procedure, efficiency, quality, scalability, sustainability) highlights the respective advantages and disadvantages of these major methods. With the development of these methods for COF membranes preparation, COFs have demonstrated exceptional performance in membrane separation applications, highlighting their substantial potential for practical implementation.

Potential strategies for scale-up preparation

Though significant advances in the fabrication of COF membranes and their impressive performance in separation, several critical challenges remain before their widespread practical implementation can be realized. Firstly, most current synthesis methods yield COF membranes with poor

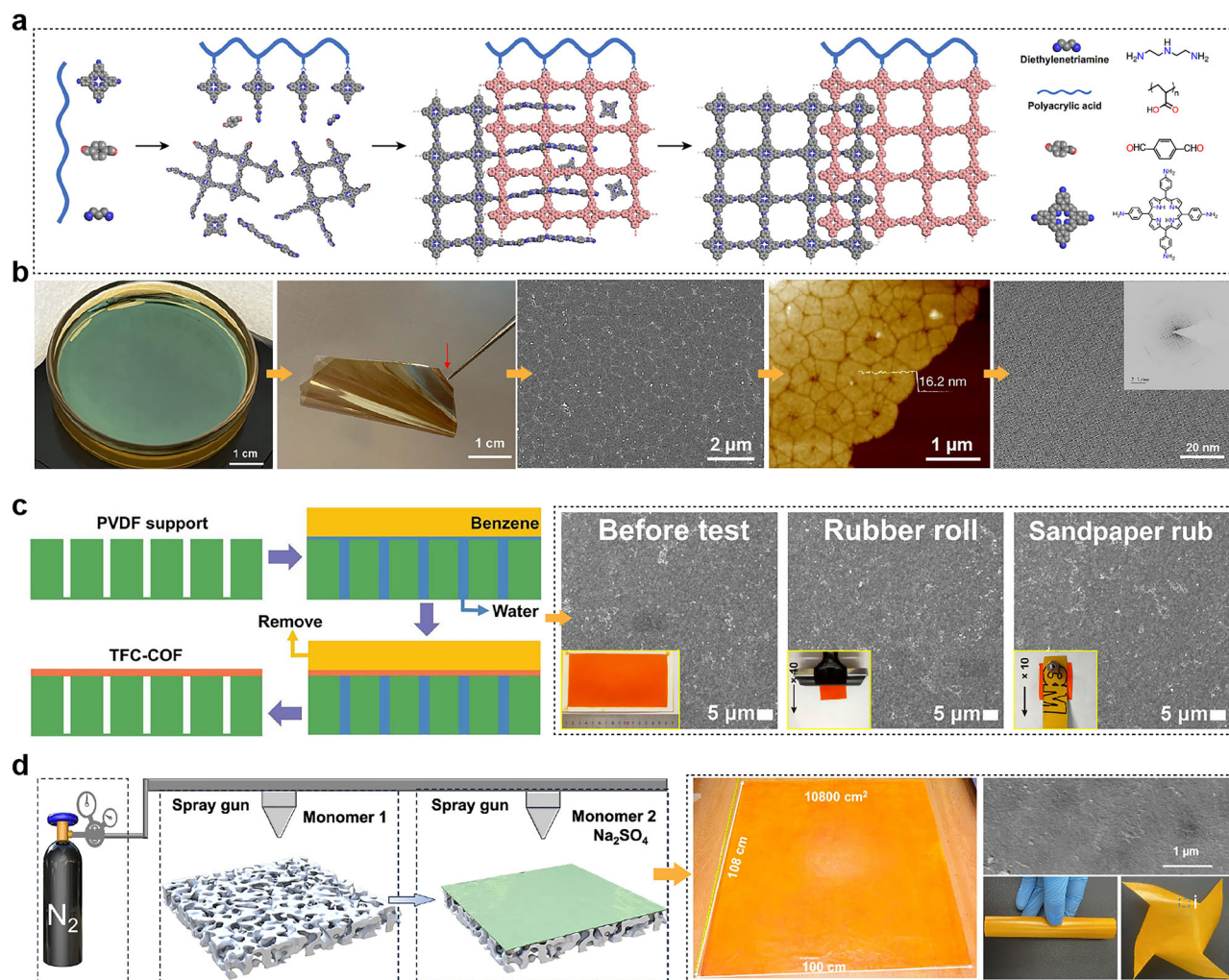


Fig. 5 | Interfacial polymerization for COF membrane preparation. **a, b** Schematic view of the polymerization and crystallization process of node and linker, and the prepared highly strong, tough, and elastic single-crystal 2D COF membranes. Polyacrylic acid as a template and diethylenetriamine as a sacrificial go-between to direct the growth and crystallization of COF membranes. Reproduced with permission from ref. 117 (copyright Springer Nature, 2024). **c** Synthesis scheme and macroscopic appearance of the TFC-COF membrane, as well as the experimental

procedures adopted to assess its mechanical robustness via rubber roller rolling and sandpaper scrubbing. The corresponding SEM images of the membrane before and after abrasion are also provided¹²¹ (copyright Elsevier, 2022). **d** Schematic of the TFC-COF membrane fabrication process, digital photos of the resulting ~ 1 m² membrane and different folding shapes, and a corresponding SEM image of the membrane. Reproduced with permission from ref. 122 (copyright Springer Nature, 2025).

crystallinity and orientation, which hinders the full exploitation of their intrinsic pore channels for separation—particularly in terms of oriented structures. Despite a few studies have reported oriented COF membranes, these successes remain difficult to generalize, primarily due to an insufficient understanding of the crystallization and orientation mechanisms underlying membrane formation, particularly for charged COF systems. Secondly, while several fabrication strategies show potential for scaling up, only a limited number of large-area COF membranes have been successfully demonstrated, and performance evaluations are still limited to small membrane areas. Finally, achieving cost-effective and environmentally sustainable manufacturing—by minimizing both production costs and the use of organic solvents—remains a major hurdle.

In recent years, with deepening research and continuous refinement of COF membrane fabrication techniques, the realization of large-area COF membranes for practical applications appears promising. For example, Sahabudeen et al.¹¹⁶ developed the SMAIS method, which employs surfactants as templates to direct the reaction of COF monomers and guide membrane formation, enabling the preparation of highly crystalline COF membranes. Yang et al.¹¹⁷ further utilized polyacrylic acid as a template and diethylenetriamine as a sacrificial go-between to direct the growth and

crystallization of COF membranes, producing highly strong, tough, and elastic single-crystal 2D COF membranes (Fig. 5a, b). These studies not only provide strategic insights into the controlled synthesis of COF membranes but also help elucidate crystallization mechanisms during interfacial polymerization, paving the way for high-quality membrane fabrication. Furthermore, interfacial polymerization—a cornerstone technique for fabricating polymer membranes (e.g., polyamide/polyester-based thin-film composite (TFC) membranes), dominates industrial separations—has been extensively adapted for the preparation of large-area COF membranes. For instance, Chen et al.¹²¹ proposed a facile interfacial method that leverages synergistic interfacial diffusion and in-phase Brownian motion to synthesize large-area COF membranes. This approach enables the formation of continuous 111 nm-thick COF films within 3 h, as well as the fabrication of TFC-structured COF membranes with areas up to 120 cm² (Fig. 5c). Similarly, Du et al.¹²² employed a spray-coating process combined with electrostatic-assisted interfacial monomer aggregation to enhance diffusion, reactivity, and competitive coordination regulation, fulfilling suitable reaction-diffusion conditions for Turing architecture. This method allowed the preparation of TFC-structured COF membranes with areas of ~ 1 m² (Fig. 5d). As process control, mechanistic understanding, and fabrication

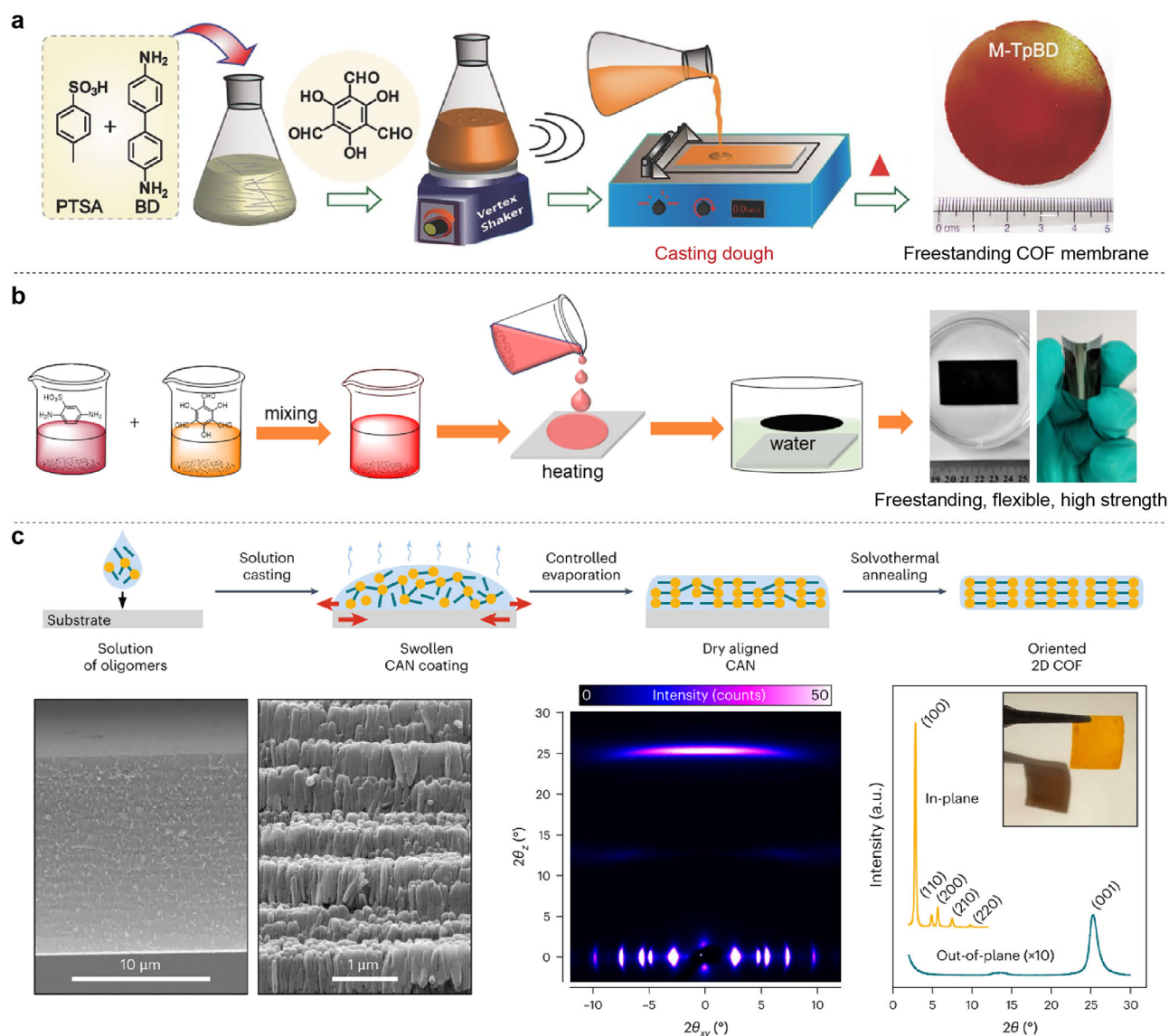


Fig. 6 | Casting method for the preparation of freestanding COF membranes. **a** Schematic representation of the freestanding COF membranes fabrication and the digital photo of the prepared M-TpBD COF membrane. Reproduced with permission from ref. 94 (copyright Wiley-VCH, 2017). **b** Schematic illustration of the process of the fabrication of freestanding COF membrane and the prepared freestanding COF membrane with flexible and high strength. The two monomers were dissolved in NMP and DMSO, respectively, to form uniform solutions. Reproduced

with permission from ref. 123 (copyright Wiley-VCH, 2021). **c** The proposed method for the preparation of oriented 2D COF films by spontaneous alignment of a CAN followed by amorphous-to-crystalline transformation. Cross-sectional SEM images, 2D GIWAXS pattern, the corresponding In-plane (near $2\theta_z = 0$) and out-of-plane (near $2\theta_{xy} = 0$) projections. Inset: camera picture of the membrane. Reproduced with permission from ref. 124 (copyright Springer Nature, 2025).

protocols for interfacial polymerization continue to mature, the scalable production of high-quality, large-area COF membranes appears increasingly attainable.

Casting methods have also evolved rapidly for fabricating freestanding COF membranes recently. In 2017, Banerjee et al.⁹⁴ demonstrated a simple “casting dough” technique to produce freestanding COF membranes (Fig. 6a). However, the heterogeneous reaction system inherently compromises membrane microstructural densification. In 2021, Hou et al.¹²³ refined this approach by dissolving COF monomers in a mixed solvents of NMP and DMSO to form a homogeneous precursor solution, followed by casting on a glass plate in the oven at 60 °C for 6 days to yield freestanding TpPa-SO₃H membrane (Fig. 6b). Nevertheless, this modified methodology remains nascent, retaining challenges such as prolonged reaction durations, insufficient process control, and unresolved membrane formation mechanisms. In 2025, Cusin et al.¹²⁴ utilized the casting method, combined with solvent evaporation and annealing processes, achieving the fabrication

of a micrometre-thick oriented 2D COF membranes by leveraging a kinetically trapped amorphous 3D covalent adaptable network (CAN) intermediate (Fig. 6c). This versatile kinetic trapping strategy is applicable to a range of building blocks and network topologies, enabling the production of 2D COF membranes with highly aligned polycrystalline structures. However, the current fabrication process is relatively complex, involves the use of large amounts of organic solvents, and has not been demonstrated for charged COF membranes, indicating a need for further optimization and in-depth investigation. It is believed that with continued refinement of this method, there are promising prospects for the production of high-quality, large-area COF membranes and their practical applications.

Ion separation

Conventional polymer membranes face a long-standing trade-off between ion permeability and selectivity. This limitation arises from their ill-defined ion-conduction pathways and poor dimensional stability, which leads to

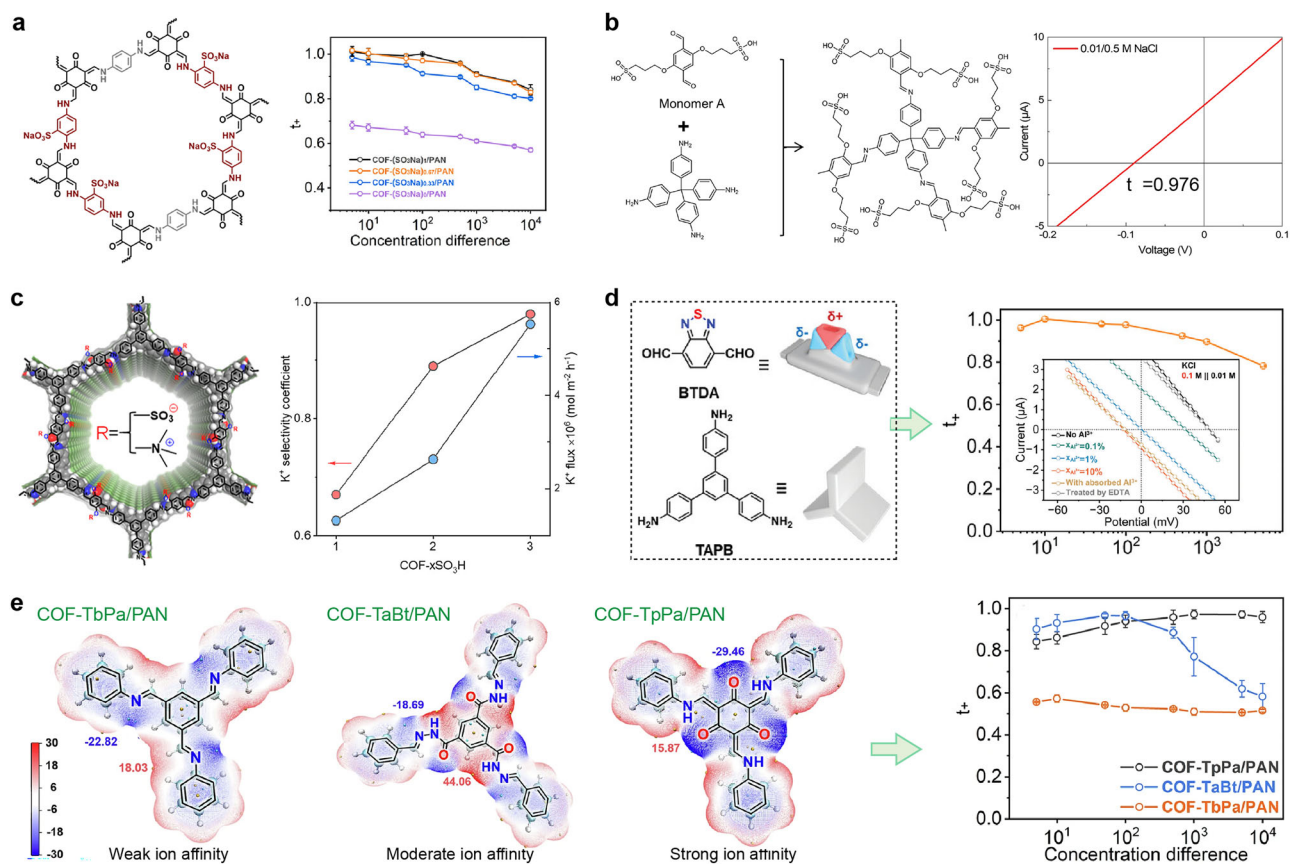


Fig. 7 | COF membranes with cations/anions selectivity for osmotic energy conversion. **a** Negative charged COF membrane with modulated charge density in the pore channels to enhance the permselectivity and ion conductance, leading to a larger osmotic voltage and current. Reproduced with permission from ref. 126 (copyright Wiley-VCH, 2022) **b** The sulfonic acid-functionalized 3D SCOF membrane deployed in osmotic energy conversion. Reproduced with permission from ref. 128 (copyright Springer Nature, 2023). **c** A pair of 100-nm-thick oriented COF membranes COF – SO₃H – x and COF – QA – x for osmotic energy conversion.

Reproduced with permission from ref. 129 (copyright American Chemical Society, 2022). **d** The COF-TAPB-BDTA membrane with aligned benzothiadiazole dipole moieties for salinity gradients energy extraction. Reproduced with permission from ref. 131 (copyright Wiley-VCH, 2024). **e** The β -ketoenamine linkage COF membrane with record permselectivity in high salinity environments employed in low-grade waste heat conversion. Reproduced with permission from ref. 132 (copyright Springer Nature, 2024).

significant swelling in solvents and consequent degradation of selectivity. In contrast, COF-based membranes have emerged as promising candidates for high-efficiency ion separation, owing to their well-defined pore structures and tailored functionalities²². The ordered channels promote fast ion transport and thus the increase of permeance, and the enhanced interactions between the ions and functionalized channel wall contribute to selective ion transport and the rising of selectivity. Consequently, a growing number of COF membranes have been reported for ion separations, breaking the trade-off limitations, including cation/anion, mono-/multivalent ion, and mono-/monovalent ion separation.

Cation/anion separation

Cations and anions can be effectively separated by traditional ion-exchange membranes (IEMs), which leverage differences in electrostatic interactions between the fixed charges in the membrane matrix and co-ions/counterions⁵. However, conventional IEMs typically form hydrophilic ion-selective channels through hydrophilic-hydrophobic phase separation. These channels are prone to significant swelling in aqueous environment, which is markedly exacerbated with increasing ion-exchange capacity (IEC) and consequently compromises cation/anion selectivity. Previous studies have indicated that enhancing the rigidity of the ion-selective channels can effectively suppress membrane swelling and thus improve separation performance, as demonstrated in polymers of intrinsic microporosity (PIMs) and triazine-based framework membranes^{4,17}. Nevertheless, the IEC values of most reported polymeric membranes, including amorphous porous

polymers such as PIMs, remain generally low. In contrast, the highly rigid and ordered frameworks of COF membranes are theoretically capable of maintaining minimal swelling even at high IEC levels, positioning them as promising materials for highly efficient cation/anion separation.

In 2021, Chen et al.¹²⁵ developed a strategy integrating ionic elements into angstrom-sized channels via in situ encapsulation of charged dyes during 3D COF interfacial polymerization. This method enabled precise guest control, yielding JGx@COF/PAN membranes with anion selectivity. Cl⁻/Mⁿ⁺ permeability ratios reached 1357 (MgCl₂), 452 (LiCl), 296 (NaCl), and 189 (KCl) under 0.1 M/1 mM gradients. Notably, the optimized JG_{80.1}@COF/PAN membrane achieved exclusive Cl⁻ transport (transport number: $t_{-} \approx 1$) below 0.1 M/0.1 mM gradients. Subsequently, Zuo et al.¹²⁶ introduced PaSO₃Na monomer to prepare negatively charged COF membranes and modulate the charge density in the pore channels to enhance the permselectivity and ion conductance, leading to a larger osmotic voltage and current. Moreover, the prepared negative COF membranes exhibited a t_{+} value of 0.8 even at a concentration difference of 10⁴ (Fig. 7a). Cao et al.¹²⁷ further employed PaSO₃H monomer to prepare in-plane-oriented COF nanosheets and assembled them into a proton-conducting membrane. The resulting membrane exhibited a high IEC of 3.2 mmol g⁻¹ and a remarkably low area swelling ratio of ~1% at both 25 °C and 80 °C. In addition, the membrane showed high proton conductivity of 0.38 S cm⁻¹ at 80 °C, with 1–2 orders of magnitude higher than that of benchmark PEMs and a weakly humidity-dependent conductivity over a wide range of humidity (30–98 %). In 2023, Zhu et al.¹²⁸ synthesized 3D sulfonated COF (3D SCOF)

membranes via dual acid-mediated interfacial polymerization (Fig. 7b), achieving a cation transport number of 0.976 and a proton conductivity of 843 mS cm^{-1} at 90°C . Cao et al.¹²⁹ developed two oriented COF membranes $\text{COF} - \text{SO}_3\text{H} - x$ and $\text{COF} - \text{QA} - x$, with cation and anion selectivity, respectively, via post-functionalization (Fig. 7c). Wang et al.¹³⁰ reported an ionic COF membrane with superhigh IEC of 4.6 mmol g^{-1} by introducing 4,4'-diaminobiphenyl-3,3'-disulfonic acid, while maintaining a low swelling ratio of $\sim 21\%$ at 25°C and a prominent proton conductivity of 0.66 S cm^{-1} . Peng et al.⁸² synthesized NUS-10 COF with a higher theoretical IEC of $\sim 5.4 \text{ mmol g}^{-1}$ by utilizing highly charged 2,5-diaminobenzene-1,4-disulfonic acid monomer, holding great promise in high-efficient cation/anion separation applications. Beyond conventional charged COF membranes, Lai et al.¹³¹ engineered COF membranes with aligned benzothiadiazole dipoles (Fig. 7d), enabling dynamic modulation of ion permselectivity across cation-selective, ambipolar, and anion-selective states by exploiting ion-dipolar interactions. When interacting with multivalent anions, the channels exhibited strong cation conductivity and permselectivity ($t_+ = 0.9$) even under a 1000-fold concentration gradient. Yin et al.¹³² modulated ion-membrane interactions through linkage chemistry (Fig. 7e), showing that charge-neutral β -ketoamine-linked COF membranes achieved record cation permselectivity under high-salinity conditions and maintained robust ion selectivity under thermal gradients ($\Delta T = 50 \text{ K}$).

Despite substantial progress in developing architecturally diverse COF membranes with exceptional cation/anion permselectivity by electrostatic, ion-dipolar, and ion-membrane interactions, critical challenges still remain. Firstly, most reported COF membranes show low crystalline and orientation, which hinders the full exploitation of their intrinsic pore channels, resulting in significant differences in the ion transport rates for similar COF membrane and noteworthy lower than the theoretical values. In addition, the performance of COF membranes was evaluated with limited area, such as the reported COF membrane with cation/anion selectivity for osmotic energy conversion only measured in 1 mm^2 membrane area. Finally, unlike traditional IEMs where electrostatic interactions dominate, ion permeation in COF nanochannels is influenced by multiple factors, including pore size, wall chemistry, and nanoconfinement effects. However, a unified theoretical framework to elucidate how these factors collectively dictate ion transport mechanisms under nanoconfinement in COFs remains absent. Therefore, it is imperative to develop scalable fabrication methods for large-area COF membranes, establishing standardized protocols for performance assessment under realistic conditions, and designing modular multi-membrane cascade systems. Furthermore, advanced characterization techniques combined with theoretical modeling are critically to gain deeper insights into the ion transport processes and underlying mechanisms within the confined nanochannels of COF membranes.

Mono-/multivalent ion separation

Compared with cation/anion separation, the separation of mono-/multivalent ions with identical charge polarity poses a substantially greater challenge. In recent years, the rapid expansion of the electric vehicle industry has drastically increased the demand for lithium resources². It is noteworthy that approximately 60% of global lithium reserves exist in Salt Lake brines, which contain high concentrations of Mg^{2+} . The similar physicochemical properties of Li^+ and Mg^{2+} make their separation a major bottleneck in lithium extraction.

Monovalent and multivalent ions carry the same charge polarity but differ in charge number, leading to marked differences in hydrated ion size and hydration energy. For instance, the hydrated diameters of Li^+ and Mg^{2+} are approximately 7.64 \AA and 8.56 \AA , respectively⁶³, while their hydration energies are about -475 kJ mol^{-1} and $-1830 \text{ kJ mol}^{-1}$. These differences provide a basis for efficient separation through precise design of pore size and channel-wall chemistry. For example, Yin et al.⁶¹ employed solvent vapor annealing to reorient COF channels from anisotropic to perpendicular alignment. The resultant TbHZ membrane with 9.8 \AA perpendicular-aligned subnanochannels achieved 2 \AA -level ion differentiation and a $\text{SO}_4^{2-}/\text{PTS}^{4-}$ selectivity of 16.8 (Fig. 8a). In 2021, our group prepared an ultrathin

($\sim 20 \text{ nm}$) TpBDME₂ COF membrane with sub-2 nm channels and abundant hydrogen-bonding sites via a counter-diffusion approach⁶³. The membrane exhibited high monovalent cation permeation rates (K^+ : $\sim 0.2 \text{ mol m}^{-2} \text{ h}^{-1}$) and outstanding mono-/multivalent cation selectivity through channel-cation hydrogen bonding interactions ($\text{K}^+/\text{Mg}^{2+}$: 765, $\text{Na}^+/\text{Mg}^{2+}$: 680, $\text{Li}^+/\text{Mg}^{2+}$: 217), breaking the permeability-selectivity trade-off for conventional ion-separation membranes (Fig. 8b)⁶³. Furthermore, the difference in charge number between mono- and multivalent ions also enables their separation by introducing electrostatic interactions in charged nanochannels. In 2024, Liu et al.⁸ introduced positively charged aldehyde monomer and synthesized an asymmetric-structured HBAB-TAPA-COF membrane on HPAN via counter-diffusion. The membrane consisted of vertically aligned nanorods that enhanced water/ion contact and an ultrathin dense layer that enabled both high permeability (Cs^+ : $0.33 \text{ mol m}^{-2} \text{ h}^{-1}$) and selectivity ($\text{Cs}^+/\text{La}^{3+}$: 75.9) (Fig. 8c). Shi et al.¹³³ engineered 3D-OH-COF membranes on cross-linked polyimide substrate through in situ growth, showing free ion permeation but effective dye rejection. Subsequent post synthesis yielded 3D-COOH-COF membranes with selective Cu^{2+} capture via chemical adsorption and electrostatic interactions, achieving $\text{K}^+/\text{Cu}^{2+}$, $\text{Na}^+/\text{Cu}^{2+}$, and $\text{Li}^+/\text{Cu}^{2+}$ selectivity of ~ 766 , ~ 634 , and ~ 490 , respectively. In 2025, Meng et al.⁷ prepared COF-300-V membranes using counter-diffusion, followed undergoing a post-modification by a click reaction to obtain COF-300-CH_{0.6} membrane. The prepared membrane exhibited a $\text{Li}^+/\text{Mg}^{2+}$ selectivity of 321 and a Li^+ flux of $0.53 \text{ mol m}^{-2} \text{ h}^{-1}$ in electro dialysis surpassing the reported PIM, COF, MOF GO, and MXene membranes, with electric-field-assisted decoupling revealing membrane charge density-transport correlations (Fig. 8d). In addition, Meng et al.¹³⁴ improved ion- π interactions with multivalent ions through optimizing the face-to-face orientation of building blocks during the assembly of COF membranes to achieve both mono-/multivalent cations and anions separation (Fig. 8e). The prepared COF-170/PAN membrane show high selectivity of 214 for $\text{K}^+/\text{Al}^{3+}$, 62 for $\text{Cl}^-/\text{SO}_4^{2-}$, and 451 for $\text{NO}_3^-/\text{PO}_4^{3-}$, which is superior to most reported polymer, GO, COF, and MOF membranes. Additionally, Afzal et al.¹³⁵ developed an SCOF-based hybrid membrane by incorporating SCOF into an SPEEK matrix for vanadium redox flow batteries. The SCOF creates a pore structure that facilitates selective proton conduction, achieving a peak $\text{H}^+/\text{VO}^{2+}$ selectivity of $\sim 6 \times 10^5 \text{ S min cm}^{-3}$ —4.5 times higher than that of Nafion 212.

Over the past five years, COF membranes have shown rapid progress in high-efficient mono-/multivalent ion separation, achieving simultaneously enhanced in monovalent ion permeability and mono-/multivalent ion selectivity. However, a deep mechanistic understanding of ion discrimination remains challenging, particularly regarding ion transport dynamics under nanoconfinement and the microscopic origin of selectivity differences. Therefore, advanced characterization techniques such as in situ spectroscopy, synchrotron radiation methods, and quasielastic neutron scattering have garnered significant attention and are being applied to the study of ion transport and separation mechanisms. For instance, Wang et al.¹³⁶ demonstrated the modulation of hydrated micropore size (less than two nanometres) enables direct control over water and ion transport across broad length scales, which quantified by quasielastic neutron scattering spectroscopic and computational methods. Zuo et al.⁴ measured the self-diffusion coefficient of Na^+ in the channel of triazine framework membranes by using ²³Na Pulsed-field Gradient (PFG)-NMR experiment at a Larmor frequency of 158.75 MHz, demonstrating near-frictionless ion transport within triazine framework membranes.

Monovalent ion separation

The separation of monovalent ions from each other presents a far greater challenge than mono-/multivalent ion separation, owing to their identical charge polarity and quantities. Research on mono-/monovalent ion separation remains limited, and the underlying mechanisms are still in the early stages of exploration. In 2022, Wang et al.¹³⁷ engineered negatively charged COF membranes via LBL assembly and demonstrated the precise separation for mono-/monovalent cations (Fig. 9a). By tailoring acidic

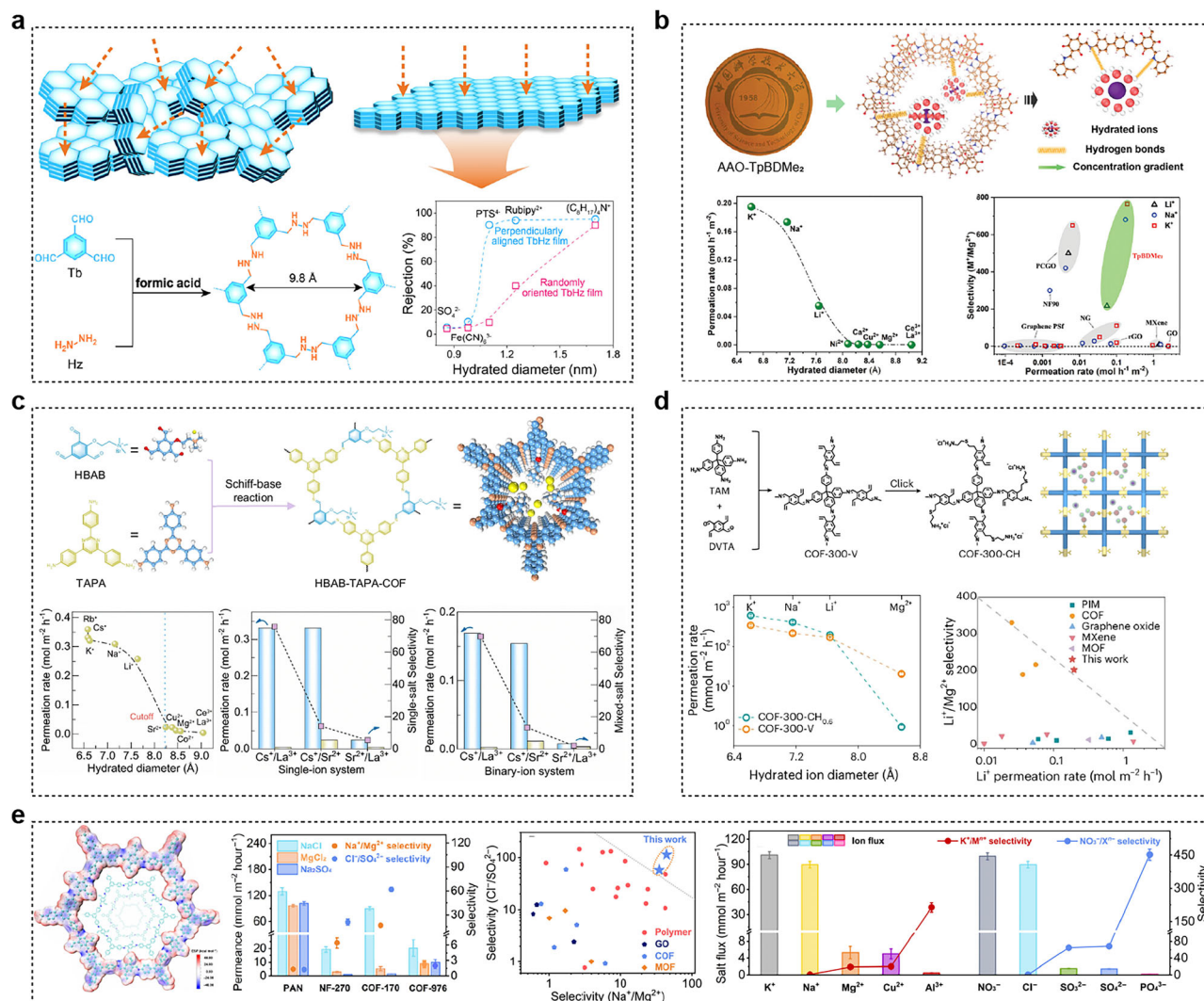


Fig. 8 | COF membranes for mono-/multivalent ion separation. **a** The preparation of perpendicularly aligned TbHZ membrane for $\text{SO}_4^{2-}/\text{PTS}^{4-}$ separation. Reproduced with permission from ref. 61 (copyright American Chemical Society, 2023). **b** Ultrathin sub-2-nanochannel COF (TpBDMe₂) membranes used for mono-/multivalent cation separation through hydrogen bonding interactions. Reproduced with permission from ref. 63 (copyright Wiley-VCH, 2021). **c** The asymmetric structure HBAB-TAPA-COF membrane employed to separate mono-/multivalent cations.

groups on COF nanochannels, the optimized TpPa-PO₃H₂ membrane achieved a K^+/Li^+ ideal selectivity of 13.7 and actual selectivity of 4.2–4.7 for K^+/Li^+ binary mixtures. Moreover, Sun et al.⁷⁸ constructed well-oriented TpHZ-D COF membranes by interfacial polymerization with organic solvent modulation (Fig. 9b). The prepared membrane demonstrates rapid and selective transport of Li^+ ions over Na^+ and K^+ ions due to the pore-entrance sieving effect and ion–channel wall interactions, achieving Li^+/K^+ and Li^+/Na^+ selectivity ratios of 38.7 and 7.2, respectively. In 2025, Wu et al.⁸³ synthesized TpPa-COOH nanosheets via oil-water-oil triphase strategy, subsequently assembling them on porous nylon substrates using dopamine-mediated LBL method. The pH-responsive dopamine spacers enabled dynamic tuning of COF pore sizes (from 1.25 to 0.71 nm), achieving a K^+/Li^+ selectivity of 18.7 (Fig. 9c). Separately, Niu et al.¹³⁸ embedded COF-300 particles into polystyrene (PS) to fabricate COF-300/PS MMMs. The well-ordered pore architecture and surface functional groups enabled selective mono/monovalent cation separation, achieving a K^+/Li^+ selectivity of 31.5 (Fig. 9d).

Though the ordered pore architectures and atomically precise tunability of channel wall chemistry in COFs endow them with immense

Reproduced with permission from ref. 8 (copyright Springer Nature, 2024). **d** The cationic COF-300-CH_{0.6} membrane deployed in $\text{Li}^+/\text{Mg}^{2+}$ separation by electro-dialysis. Reproduced with permission from ref. 7 (copyright Springer Nature, 2025). **e** The COF-170/PAN membrane with improved ionπ interactions for both mono-/multivalent cation and anion separation. Reproduced with permission from ref. 134 (copyright American Association for the Advancement of Science).

potential for precise ion discrimination, the development of COF membranes for precise mono/monovalent ion separation is still in its infancy. Both separation performance and mechanistic understanding require further in-depth investigation. First, the precision in fabricating COF membranes needs to be optimized. Combining advanced microscopic characterization and in situ analysis can provide deeper insights into crystallization and growth mechanisms, enabling the synthesis of highly crystalline and oriented COF membranes. This will lay a solid foundation for investigating ion transport mechanisms. Second, systematic exploration of membrane microstructure is essential. Although numerous gCOF architectures—including varied pore geometries, dual- and multi-pore systems, and tunable pore sizes and microenvironments—have been developed, only a limited subset have been realized as membranes. Future efforts should focus on designing COF membranes with more precisely engineered pore structures, quantitatively correlating key microstructural parameters with ion transport and selectivity, and evaluating the contribution of each structural factor to ion permeation rates. Finally, beyond mono/monovalent cation separation, the precise separation of mono/monovalent anions and other isoivalent ions—such as rare-earth ions or isotopic ions—

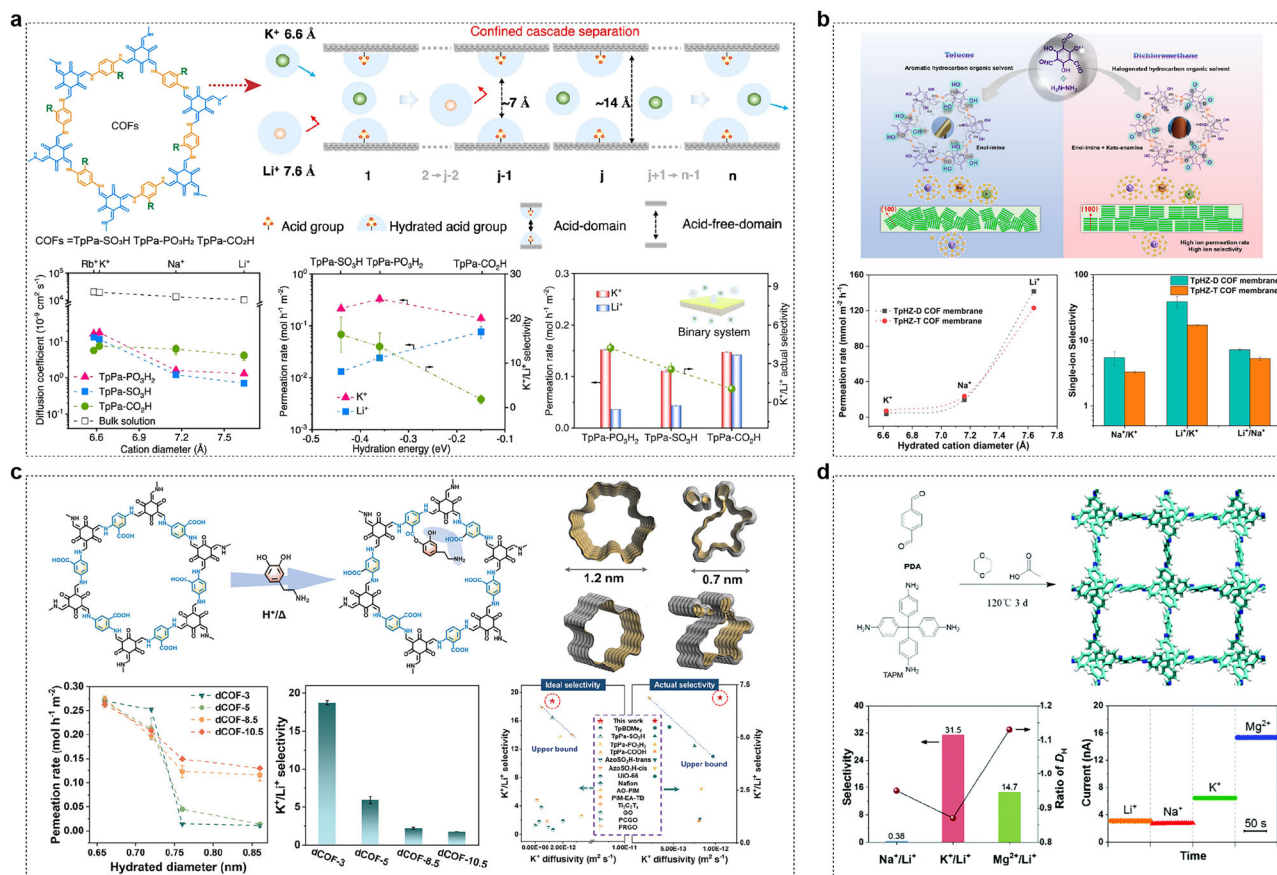


Fig. 9 | COF membrane for mono-/monovalent cations separation. **a** The modulation of acidic groups on COF nanochannels for precise separation between monovalent cations. Reproduced with permission from ref. 137 (copyright Springer Nature, 2022). **b** The construction of well-oriented TpHZ-D COF membranes through interfacial polymerization with organic solvent modulation for mono-/monovalent cation separation. Reproduced with permission from ref. 78 (copyright

American Chemical Society, 2024). **c** Acid treatment induced monomolecular dopamine to partition 1D in-plane pores of COF membrane, enabling precise separation of mono-/monovalent cation. Reproduced with permission from ref. 83 (copyright Wiley-VCH, 2025). **d** The COF-300/PS MMMs embedded COF-300 particles within polystyrene (PS) for mono-/monovalent cation separation. Reproduced with permission from ref. 138 (copyright Royal Society of Chemistry, 2022).

holds substantial scientific value and practical promise, opening new frontiers for COF-based separation technologies.

Comparison between COF and other membrane materials

COF membranes have garnered considerable research attention for ion separation due to their well-ordered pore structures, high porosity, and atomic-scale precision in pore wall engineering, establishing them as highly competitive candidates for next-generation ion-selective membranes. As illustrated in Fig. 10a, the Li^+ flux and $\text{Li}^+/\text{Mg}^{2+}$ selectivity of various membrane materials—including conventional polymer membranes, commercial ion-exchange membranes, emerging 2D material membranes, MOF membranes, and COF membranes—are compared under both diffusion and electro-driven processes^{7,62,63,72,81,105,139–142}. Among these, COF membranes demonstrate superior performance in both Li^+ flux and $\text{Li}^+/\text{Mg}^{2+}$ selectivity. Continued advances in fabrication techniques and enhanced control over crystallinity and orientation are expected to further improve their separation performance. In addition, significant progress has also been made in the precise construction of bioinspired COF membranes and the realization of smart, selective ion transport. For instance, Ren et al.⁸⁵ developed azobenzene-functionalized COF-Azo membranes via a biomimetic nanochannel modulation (BNM) strategy, forming charged and photo-switchable sub-nanochannels (Fig. 10b). Under specific light irradiation, these membranes exhibited high selectivity for both mono-/monovalent (K^+/Li^+ : 17.9) and mono-/divalent ($\text{Li}^+/\text{Mg}^{2+}$: 24.9) ion pairs, achieved through reversible angstrom-level pore size modulation via photoisomerization. In 2025, Wang et al.¹⁴¹ reported an artificial nanochannel

system based on a phase-reversed mixed-matrix COF (PRCOF) membrane incorporating localized ion-trapping sites (Fig. 10c). These sites provide moderate binding affinity and supplementary repulsive interactions, enabling precise recognition and facilitated transport of Li^+ ions. By fine-tuning the micro-environment of these traps, a high $\text{Li}^+/\text{Mg}^{2+}$ selectivity of 190 and a Li^+ permeation rate of $0.262 \text{ mol h}^{-1} \text{ m}^{-2}$ were attained in a binary mixture. In another study, Meng et al.⁶⁶ designed a triazine-based COF membrane with a suitably hydrophilic channel environment that promotes Li^+ dissociation from negatively charged functional groups, facilitating Li^+ migration via a hopping mechanism along sulfonic acid chains and thus shortening the diffusion path. In contrast, partially dehydrated Mg^{2+} , with its stronger effective charge, becomes trapped in energy wells. This mechanism mimics the selectivity of biological K^+ channels, allowing rapid Li^+ permeation while nearly completely blocking Mg^{2+} (Fig. 10d).

Long-term stability under chemical, thermal, and mechanical stresses is essential for the practical deployment of COF membranes. Although imine-linked COFs generally exhibit good hydrolytic stability, their inherent dynamic covalent chemistry often leads to degradation under strongly acidic conditions due to the reversible nature of the imine ($\text{C}=\text{N}$) bond²². Recent efforts have focused on designing COF structures resistant to harsh environments, particularly concentrated acids. For instance, Halder et al.¹¹⁸ introduced interlayer $\text{C}-\text{H}\cdots\text{N}$ hydrogen bonding and a hydrophobic microenvironment around the $\text{C}=\text{N}$ bonds, providing steric protection that ensures exceptional stability even in strongly acidic (e.g., 18 M H_2SO_4 , 12 M HCl) and alkaline (9 M NaOH), enabling effective sulfuric acid recovery. Ren et al.¹⁴³ utilized an intramolecular Povarov reaction to postsynthetically

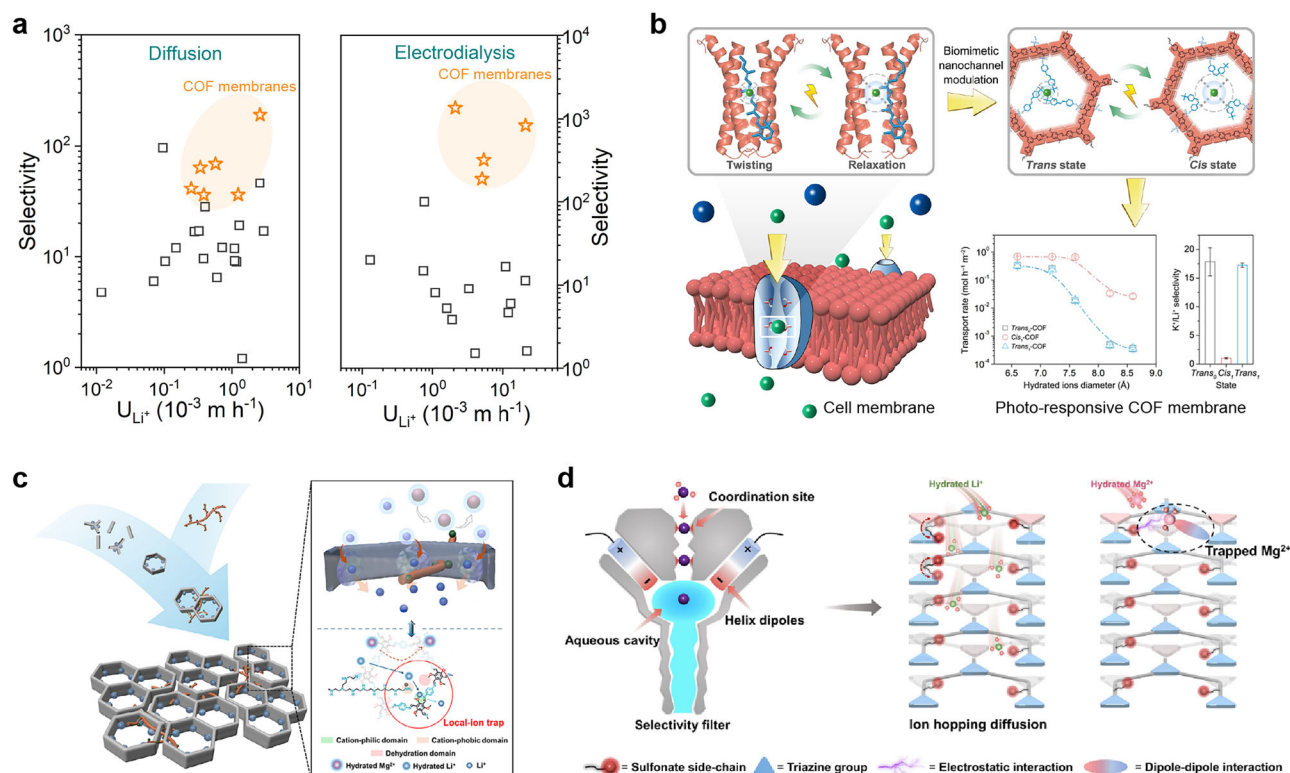


Fig. 10 | COF membrane with precise and smart nanochannels for ion separation.

a Comparison of $\text{Li}^+/\text{Mg}^{2+}$ separation performance between COF and other membrane materials^{7,62,63,72,81,105,139–142}. **b** Biomimetic construction of smart nanochannels COF membranes functionalized with photoresponsive azobenzene derivatives (COF-Azo) for precise ion separation through reversible channel gating. Reproduced with permission from ref. 85 (copyright Elsevier, 2024). **c** Schematic

illustration of phase-reversed mixed matrix covalent organic framework membrane and local-ion trap for ion separation. Reproduced with permission from ref. 141 (copyright Wiley-VCH, 2025). **d** Mechanism of ultrafast transport of K^+ in K^+ channels and biomimetic TAT-TP-P COF membrane for fast hopping transport of Li^+ , while Mg^{2+} is trapped in the energy well. Reproduced with permission from ref. 66 (copyright Wiley-VCH, 2025).

convert imine bonds into more stable chromenoquinoline linkages, yielding COFs with outstanding chemical resistance toward strong acids, bases, and oxidizing agents. Yang et al.¹⁴⁴ developed a cationic COF membrane with gradient charge distribution, which retained its structural integrity after soaking in 1 M HCl for 15 days and maintained consistent dialysis performance over ten consecutive tests. Meng et al.⁶⁶ reported a triazine-based COF membrane capable of stable $\text{Li}^+/\text{Mg}^{2+}$ separation for nearly 100 hours. More recently, Yu et al.¹⁴⁵ fabricated COF-based thin-film composite membranes within 10 min by coating COF oligomers onto poly(ether ether ketone) ultrafiltration supports. The resulting membranes exhibited stable operation for 150 h in cross-flow devices, along with excellent anti-fouling properties, showing negligible dye adsorption after 7 days of exposure to Direct Red 23. Despite these advances, most stability tests remain limited to laboratory-scale conditions and relatively short durations. Furthermore, studies on the mechanical properties of COF membranes are scarce. Although freestanding COF membranes have been prepared via methods such as interfacial polymerization, their mechanical strength remains insufficient and falls far short of industrial requirements. Therefore, further improvements in operational stability—particularly mechanical robustness under demanding conditions—are critically needed to enable real-world implementation.

Biological ion-selective channels exhibit exceptional efficiency, intelligence, and precision in ion transport. For example, K^+ channels achieve specificity through funnel-shaped architectures and coordination with carbonyl oxygens, whereas Na^+ channels utilize four carboxyl groups to confer Na^+ selectivity^{3,146}. Inspired by these natural paradigms, the construction of artificial nanochannels has emerged as a vibrant research frontier. COFs offer unique advantages in this regard, owing to their structural controllability and chemical tailorability, making them ideal platforms for developing bioinspired membranes for precision ion

separation. Consequently, developing COF-based biomimetic membranes for precision ion separation represents a promising research direction with transformative implications. Moreover, through the precise construction of bioinspired COF membranes, it is possible to investigate the mechanisms underlying highly selective ion transport, establish clear structure-property relationships between the microscopic structural parameters of COF nanochannels and their ion separation performance, and build comprehensive databases correlating structure with ion transport behavior. Notably, with the rapid advancement of artificial intelligence (AI) and the Materials Genome Initiative (MGI) has accelerated the exploration of advanced materials. By developing computational tools that predict structure-property relationships and employing materials genomics strategies, we can analyze the COF structural database and perform computational screening to enable the high-efficiency design of high-performance COF structures.

Outlook

In summary, this review presents a comprehensive overview on the research advancements, challenges, and prospects of COFs as new-generation ion-selective membranes for precise ion separation from three aspects: (i) the structural design of COFs, (ii) the preparation methods of COF membranes, and (iii) the application of COF membranes in ion separation. Regarding structural design, the discussion is organized around two fundamental perspectives: skeletal architecture and pore engineering. For membrane fabrication, we trace three evolutionary stages: from the initial discovery of COF materials, through early exploratory studies in membrane separation, to the recent rapid advancement in membrane technologies. A systematic evaluation of prevailing fabrication methods is presented using the PEQSS framework (Procedure, Efficiency, Quality, Scalability, Sustainability), followed by an in-depth discussion of viable scale-up strategies. In terms of ion

separation applications, we categorize current implementations into three groups: cation/anion separation, mono-/multivalent ion separation, and mono-/monovalent ion separation. We also present a performance comparison between COF membranes and other membrane materials for ion separation, as well as a discussion on recent advances and promising directions in bioinspired COF membranes for precise and smart ion separation. To accelerate the development of COF membranes in ion separation, several challenges are worth considering:

(1) Crystallization-controlled membrane formation mechanism of COFs

Despite significant advances having been made in developing structurally diverse COF membranes for ion separation—with their exceptional performance positioning them as highly competitive candidates for next-generation ion-selective membranes compared to conventional polymers, commercial ion-exchange membranes, emerging 2D materials, and MOFs—the current understanding of the crystallization-controlled membrane formation process and underlying mechanisms remains limited. The principles governing the modulation of COF crystallinity, orientation, and stacking modes are still poorly understood, leading to the widespread issue of low crystallinity and poor orientation in most reported COF membranes. This structural imperfection hinders the full utilization of their intrinsic pore channels, resulting in significant variability in ion transport rates even among structurally similar COF membranes, and is obviously lower than the theoretical values. Therefore, it is essential to systematically investigate the crystallization-controlled formation mechanism of COF membranes. Research in this direction should focus on understanding and regulating the crystallization process during membrane fabrication, investigating nucleation and crystal growth pathways to achieve highly ordered nanostructures, developing advanced synthesis techniques such as temperature-programmed synthesis and asymmetric monomer design, and establishing processing-structure-property relationships for separation performance optimization. A fundamental understanding of the crystallization-guided formation mechanism will significantly advance the preparation and practical implementation of highly crystalline and well-oriented COF membranes. Such structural control is expected to fully unlock their potential for efficient ion separation and further enhance their separation performance and precision.

(2) Green fabrication and evaluation of large-area COF membranes

Although various methods have been developed to fabricate COF membranes, they often involve complex procedures, prolonged reaction times, harsh synthesis conditions, and/or substantial organic solvent consumption. Coupled with the high cost of organic monomers, these limitations significantly hinder the scalable production of COF membranes. Furthermore, performance evaluations in current studies are typically conducted on small-area samples, which does not reflect the requirements for practical applications where adequate membrane area is essential for achieving high production efficiency. Moreover, insufficient long-term operational stability remains another critical barrier to real-world implementation, given that practical separation conditions often demand robustness under chemical, thermal, and mechanical stresses. Therefore, it is imperative to develop simpler and greener preparation methods for COF membranes, optimize fabrication protocols, reduce the costs associated with both monomers and processes, and systematically evaluate the performance and long-term stability of large-area membranes. Key strategies toward these goals include the development of solvent-minimized and energy-efficient synthesis routes, the establishment of standardized protocols for assessing permeability, selectivity, and long-term stability, and the implementation of life cycle assessment and green chemistry metrics for process evaluation.

(3) Bioinspired ion transport mechanisms in COF membranes

Biological ion-selective channels exhibit remarkable efficiency, intelligence, and precision in regulating ion transport. COF membranes, with their well-defined and atomically tunable pore structures, offer an ideal platform for constructing bioinspired artificial nanochannels. Consequently, developing COF-based biomimetic membranes for precision ion

separation represents a promising research direction with transformative potential. Key strategies in this field include: designing heterogeneous nanochannels inspired by biological protein structures (e.g., K^+ , Na^+ , Cl^- , and F^- channels); engineering stimuli-responsive COF membranes with gating functionality; investigating confined ion transport phenomena and selectivity mechanisms; and achieving exceptional ion selectivity through synergistic optimization of pore geometry and surface chemistry. Notably, bioinspired COF membranes are expected to substantially advance our understanding of ion transport mechanisms under nanoconfinement and guide the rational design of highly efficient membranes for precise ion separation. This is particularly critical for challenging separations involving ions with minimal physicochemical differences. For instance, hydrated K^+ (6.62 Å) and Na^+ (7.16 Å) exhibit a diameter difference of merely 0.54 Å, while hydrated Ce^{3+} and La^{3+} possess identical diameters of 9.04 Å. Similarly, isotopic ${}^6Li^+$ and ${}^7Li^+$ demonstrate nearly indistinguishable characteristics. Achieving high-precision separation between such ion pairs necessitates elucidation of their selective transport mechanisms at the atomic level. To this end, complementary approaches beyond nanochannel engineering are required. Advanced characterization techniques—such as in situ spectroscopy, synchrotron radiation analysis, and quasi-elastic neutron scattering—are essential for resolving dynamic ion transport behavior within confined spaces. The integration of bioinspired design with sophisticated experimental probes will establish a fundamental framework for the next generation of ion-selective membranes.

(4) AI-assisted computational screening and structural design

The rational design and development of high-performance COF membranes for ion separation fundamentally rely on clarifying the key microstructural parameters governing ion transport. These include pore size, channel geometry, surface hydrophilicity/hydrophobicity, and specific interactions between functional groups and ions—such as electrostatic, hydrogen bonding, coordination, and ion-dipole interactions—particularly the synergistic effects among these factors under nanoconfinement. However, a unified theoretical framework to elucidate how these parameters collectively dictate ion transport mechanisms in the confined nanochannels of COFs remains absent. A deep understanding of the structure-property relationships between the microscopic features of COF pores and their ion separation performance requires extensive material synthesis and accurate performance evaluation, which poses considerable experimental and theoretical challenges. In recent years, the rapid development of AI and the widespread adoption of the MGI have greatly accelerated the exploration of advanced functional materials. By building computational tools capable of predicting structure-property relationships and implementing materials genomics strategies, it becomes feasible to systematically analyze existing COF structural databases, perform high-throughput computational screening, and enable efficient design of high-performance COF membranes. Such approaches will help establish clear correlations between nanochannel microstructural parameters and ion separation behavior, while also constructing comprehensive databases that link COF architecture with ion transport performance.

Data availability

This paper discusses original data from publications cited throughout the paper.

Received: 25 June 2025; Accepted: 11 December 2025;

Published online: 09 January 2026

References

1. Uliana, A. A. et al. Ion-capture electro dialysis using multifunctional adsorptive membranes. *Science* **372**, 296–299 (2021).
2. Razmjou, A., Asadnia, M., Hosseini, E., Habibnejad Korayem, A. & Chen, V. Design principles of ion selective nanostructured membranes for the extraction of lithium ions. *Nat. Commun.* **10**, 5793 (2019).

3. Noskov, S. Y., Bernèche, S. & Roux, B. Control of ion selectivity in potassium channels by electrostatic and dynamic properties of carbonyl ligands. *Nature* **431**, 830–834 (2004).
4. Zuo, P. et al. Near-frictionless ion transport within triazine framework membranes. *Nature* **617**, 299–305 (2023).
5. Ran, J. et al. Ion exchange membranes: new developments and applications. *J. Membr. Sci.* **522**, 267–291 (2017).
6. Chen, Y., Zhu, Z., Tian, Y. & Jiang, L. Rational ion transport management mediated through membrane structures. *Exploration* **1**, 20210101 (2021).
7. Meng, W. et al. Three-dimensional cationic covalent organic framework membranes for rapid and selective lithium extraction from saline water. *Nat. Water* **3**, 191–200 (2025).
8. Liu, Q. et al. Covalent organic framework membranes with vertically aligned nanorods for efficient separation of rare metal ions. *Nat. Commun.* **15**, 9221 (2024).
9. Song, W. et al. Upscaled production of an ultramicroporous anion-exchange membrane enables long-term operation in electrochemical energy devices. *Nat. Commun.* **14**, 2732 (2023).
10. Wu, Y. et al. Crystallizing self-standing covalent organic framework membranes for ultrafast proton transport in flow batteries. *Angew. Chem. Int. Ed.* **62**, e202313571 (2023).
11. Shin, D. W., Guiver, M. D. & Lee, Y. M. Hydrocarbon-based polymer electrolyte membranes: importance of morphology on ion transport and membrane stability. *Chem. Rev.* **117**, 4759–4805 (2017).
12. Kusoglu, A. & Weber, A. Z. New insights into perfluorinated sulfonic-acid ionomers. *Chem. Rev.* **117**, 987–1104 (2017).
13. Zhang, J. et al. Cation–dipole interaction that creates ordered ion channels in an anion exchange membrane for fast OH[−] conduction. *AIChE J.* **67**, e17133 (2021).
14. Shen, J., Liu, G., Han, Y. & Jin, W. Artificial channels for confined mass transport at the sub-nanometre scale. *Nat. Rev. Mater.* **6**, 294–312 (2021).
15. Tan, L. & Tan, B. Hypercrosslinked porous polymer materials: design, synthesis, and applications. *Chem. Soc. Rev.* **46**, 3322–3356 (2017).
16. Tan, R. et al. Hydrophilic microporous membranes for selective ion separation and flow-battery energy storage. *Nat. Mater.* **19**, 195–202 (2020).
17. Zuo, P. et al. Sulfonated microporous polymer membranes with fast and selective ion transport for electrochemical energy conversion and storage. *Angew. Chem. Int. Ed.* **59**, 9564–9573 (2020).
18. Xu, Y., Jin, S., Xu, H., Nagai, A. & Jiang, D. Conjugated microporous polymers: design, synthesis and application. *Chem. Soc. Rev.* **42**, 8012–8031 (2013).
19. Chen, L. et al. Ion sieving in graphene oxide membranes via cationic control of interlayer spacing. *Nature* **550**, 380–383 (2017).
20. Nair, R. R., Wu, H. A., Jayaram, P. N., Grigorieva, I. V. & Geim, A. K. Unimpeded permeation of water through helium-leak-tight graphene-based membranes. *Science* **335**, 442–444 (2012).
21. Zhang, C., Wu, B. H., Ma, M. Q., Wang, Z. & Xu, Z. K. Ultrathin metal/covalent-organic framework membranes towards ultimate separation. *Chem. Soc. Rev.* **48**, 3811–3841 (2019).
22. Wu, C., Xia, L., Xia, S., Van der Bruggen, B. & Zhao, Y. Advanced covalent organic framework-based membranes for recovery of ionic resources. *Small* **19**, 2206041 (2023).
23. Meng, Q. W., Wu, D., Wang, S. & Sun, Q. Function-led design of covalent-organic-framework membranes for precise ion separation. *Chem. Eur. J.* **29**, e202302460 (2023).
24. Yuan, S. et al. Covalent organic frameworks for membrane separation. *Chem. Soc. Rev.* **48**, 2665–2681 (2019).
25. Zhang, W., Zhang, L., Zhao, H., Li, B. & Ma, H. A two-dimensional cationic covalent organic framework membrane for selective molecular sieving. *J. Mater. Chem. A* **6**, 13331–13339 (2018).
26. Jin, Y. H., Li, M. H. & Yang, Y. W. Covalent organic frameworks for membrane separation. *Adv. Sci.* **12**, 2412600 (2025).
27. Côté, A. P. et al. Porous, crystalline, covalent organic frameworks. *Science* **310**, 1166–1170 (2005). Yaghi et al. reported the first synthesis of crystalline porous organic frameworks (COFs): COF-1 with boroxine linkages and COF-5 with boronate ester linkages.
28. Wang, H. et al. Organic molecular sieve membranes for chemical separations. *Chem. Soc. Rev.* **50**, 5468–5516 (2021).
29. Liu, R. et al. Covalent organic frameworks: an ideal platform for designing ordered materials and advanced applications. *Chem. Soc. Rev.* **50**, 120–242 (2021).
30. Kandambeth, S., Dey, K. & Banerjee, R. Covalent organic frameworks: chemistry beyond the structure. *J. Am. Chem. Soc.* **141**, 1807–1822 (2019).
31. Chen, X. et al. Covalent organic frameworks: chemical approaches to designer structures and built-in functions. *Angew. Chem. Int. Ed.* **59**, 5050–5091 (2019).
32. Colson, J. W. et al. Oriented 2D covalent organic framework thin films on single-layer graphene. *Science* **332**, 228–231 (2011). The first COF membrane supported on single-layer graphene was prepared via an in situ growth method.
33. Fang, Q. et al. Designed synthesis of large-pore crystalline polyimide covalent organic frameworks. *Nat. Commun.* **5**, 4503 (2014).
34. Fang, Q. et al. 3D porous crystalline polyimide covalent organic frameworks for drug delivery. *J. Am. Chem. Soc.* **137**, 8352–8355 (2015).
35. Stewart, D. et al. Stable and ordered amide frameworks synthesised under reversible conditions, which facilitate error checking. *Nat. Commun.* **8**, 1102 (2017).
36. Zhang, B. et al. Crystalline dioxin-linked covalent organic frameworks from irreversible reactions. *J. Am. Chem. Soc.* **140**, 12715–12719 (2018).
37. Jackson, K. T., Reich, T. E. & El-Kaderi, H. M. Targeted synthesis of a porous borazine-linked covalent organic framework. *Chem. Commun.* **48**, 8823–8825 (2012).
38. Du, Y. et al. Ionic covalent organic frameworks with spiroborate linkage. *Angew. Chem. Int. Ed.* **55**, 1737–1741 (2015).
39. Hunt, J. R., Doonan, C. J., LeVangie, J. D., Côté, A. P. & Yaghi, O. M. Reticular synthesis of covalent organic borosilicate frameworks. *J. Am. Chem. Soc.* **130**, 11872–11873 (2008).
40. Uribe-Romo, F. J. et al. A crystalline imine-linked 3-D porous covalent organic framework. *J. Am. Chem. Soc.* **131**, 4570–4571 (2009).
41. Ding, S.-Y. et al. Construction of covalent organic framework for catalysis: Pd/COF-LZU1 in Suzuki–Miyaura coupling reaction. *J. Am. Chem. Soc.* **133**, 19816–19822 (2011).
42. Chen, X., Addicoat, M., Irlé, S., Nagai, A. & Jiang, D. Control of crystallinity and porosity of covalent organic frameworks by managing interlayer interactions based on self-complementary π–electronic force. *J. Am. Chem. Soc.* **135**, 546–549 (2012).
43. Dalapati, S. et al. An azine-linked covalent organic framework. *J. Am. Chem. Soc.* **135**, 17310–17313 (2013).
44. Fan, H. et al. Covalent organic framework–covalent organic framework bilayer membranes for highly selective gas separation. *J. Am. Chem. Soc.* **140**, 10094–10098 (2018).
45. Uribe-Romo, F. J., Doonan, C. J., Furukawa, H., Oisaki, K. & Yaghi, O. M. Crystalline covalent organic frameworks with hydrazine linkages. *J. Am. Chem. Soc.* **133**, 11478–11481 (2011).
46. Kuhn, P., Antonietti, M. & Thomas, A. Porous, covalent triazine-based frameworks prepared by ionothermal synthesis. *Angew. Chem. Int. Ed.* **47**, 3450–3453 (2008).
47. Bojdys, M. J., Jeromenok, J., Thomas, A. & Antonietti, M. Rational extension of the family of layered, covalent, triazine-based frameworks with regular porosity. *Adv. Mater.* **22**, 2202–2205 (2010).

48. Wei, P.-F. et al. Benzoxazole-linked ultrastable covalent organic frameworks for photocatalysis. *J. Am. Chem. Soc.* **140**, 4623–4631 (2018).
49. Nagai, A. et al. A squaraine-linked mesoporous covalent organic framework. *Angew. Chem. Int. Ed.* **52**, 3770–3774 (2013).
50. Beaudoin, D., Maris, T. & Wuest, J. D. Constructing monocrystalline covalent organic networks by polymerization. *Nat. Chem.* **5**, 830–834 (2013).
51. Das, G. et al. Viologen-based conjugated covalent organic networks via Zincke reaction. *J. Am. Chem. Soc.* **139**, 9558–9565 (2017).
52. Kandambeth, S. et al. Construction of crystalline 2D covalent organic frameworks with remarkable chemical (acid/base) stability via a combined reversible and irreversible route. *J. Am. Chem. Soc.* **134**, 19524–19527 (2012).
53. Fang, Q. et al. 3D microporous base-functionalized covalent organic frameworks for size-selective catalysis. *Angew. Chem. Int. Ed.* **53**, 2878–2882 (2014).
54. Chandra, S. et al. Chemically stable multilayered covalent organic nanosheets from covalent organic frameworks via mechanical delamination. *J. Am. Chem. Soc.* **135**, 17853–17861 (2013).
55. Rao, M. R., Fang, Y., De Feyter, S. & Perepichka, D. F. Conjugated covalent organic frameworks via Michael addition–elimination. *J. Am. Chem. Soc.* **139**, 2421–2427 (2017).
56. Guo, J. et al. Conjugated organic framework with three-dimensionally ordered stable structure and delocalized π clouds. *Nat. Commun.* **4**, 2736 (2013).
57. Zhuang, X. et al. A two-dimensional conjugated polymer framework with fully sp^2 -bonded carbon skeleton. *Polym. Chem.* **7**, 4176–4181 (2016).
58. Jin, E. et al. Two-dimensional sp^2 carbon–conjugated covalent organic frameworks. *Science* **357**, 673–676 (2017).
59. Dey, K. et al. Selective molecular separation by interfacially crystallized covalent organic framework thin films. *J. Am. Chem. Soc.* **139**, 13083–13091 (2017). Banerjee et al. developed interfacial polymerization as a key strategy for synthesizing freestanding imine-linked COF membranes, thereby accelerating the rapid advancement of COFs in membrane applications.
60. Cao, L. et al. Oriented two-dimensional covalent organic framework membranes with high ion flux and smart gating nanofluidic transport. *Angew. Chem. Int. Ed.* **61**, e202113141 (2022).
61. Yin, C. et al. Perpendicular alignment of covalent organic framework (COF) pore channels by solvent vapor annealing. *J. Am. Chem. Soc.* **145**, 11431–11439 (2023).
62. Meng, Q.-W. et al. Enhancing ion selectivity by tuning solvation abilities of covalent organic framework membranes. *Proc. Natl. Acad. Sci. USA.* **121**, e2316716121 (2024).
63. Sheng, F. et al. Efficient ion sieving in covalent organic framework membranes with sub-2-nanometer channels. *Adv. Mater.* **33**, e2104404 (2021). Our group fabricated an ultrathin (~20 nm) TpBDMe₂ COF membrane featuring sub-2 nm channels and abundant hydrogen-bonding sites, which achieves highly efficient mono-/multivalent cation separation.
64. Sheng, F. et al. Covalent organic framework membranes for acid recovery: The effect of charges. *Chem. Eng. J.* **462**, 142304 (2023).
65. Zhu, R. et al. Fabrication of synergistic sites on an oxygen-rich covalent organic framework for efficient removal of Cd(II) and Pb(II) from water. *J. Hazard. Mater.* **424**, 127301 (2022).
66. Meng, W. et al. Dehydration-enhanced ion recognition of triazine covalent organic frameworks for high-resolution Li^+/Mg^{2+} separation. *Angew. Chem. Int. Ed.* **64**, e202422423 (2025).
67. Nagai, A. et al. Pore surface engineering in covalent organic frameworks. *Nat. Commun.* **2**, 536 (2011).
68. Mitra, S. et al. Self-exfoliated guanidinium-based ionic covalent organic nanosheets (iCONs). *J. Am. Chem. Soc.* **138**, 2823–2828 (2016).
69. Dalapati, S. et al. Rational design of crystalline supermicroporous covalent organic frameworks with triangular topologies. *Nat. Commun.* **6**, 7786 (2015).
70. Ding, X. et al. Synthesis of metallophthalocyanine covalent organic frameworks that exhibit high carrier mobility and photoconductivity. *Angew. Chem. Int. Ed.* **50**, 1289–1293 (2011).
71. Chen, X. et al. Designed synthesis of double-stage two-dimensional covalent organic frameworks. *Sci. Rep.* **5**, 14650 (2015).
72. Meng, Q.-W. et al. Regulation of ion binding sites in covalent organic framework membranes for enhanced selectivity under high ionic competition. *ACS Nano* **19**, 12080–12089 (2025).
73. Li, Y. et al. Laminated self-standing covalent organic framework membrane with uniformly distributed subnanopores for ionic and molecular sieving. *Nat. Commun.* **11**, 599 (2020).
74. Pang, Z. F. et al. Construction of covalent organic frameworks bearing three different kinds of pores through the heterostructural mixed linker strategy. *J. Am. Chem. Soc.* **138**, 4710–4713 (2016).
75. Qian, C. et al. Toward covalent organic frameworks bearing three different kinds of pores: The strategy for construction and COF-to-COF transformation via heterogeneous linker exchange. *J. Am. Chem. Soc.* **139**, 6736–6743 (2017).
76. Liang, R.-R. et al. Rational design of crystalline two-dimensional frameworks with highly complicated topological structures. *Nat. Commun.* **10**, 4609 (2019).
77. Wang, R. et al. Green and large-scale production of covalent organic framework nanofiltration membranes. *Commun. Mater.* **6**, 61 (2025).
78. Sun, Q. et al. Covalent organic framework membranes with regulated orientation for monovalent cation sieving. *ACS Nano* **18**, 27065–27076 (2024).
79. Mu, Z. et al. Covalent organic frameworks with record pore apertures. *J. Am. Chem. Soc.* **144**, 5145–5154 (2022).
80. Ma, H. et al. Cationic covalent organic frameworks: a simple platform of anionic exchange for porosity tuning and proton conduction. *J. Am. Chem. Soc.* **138**, 5897–5903 (2016).
81. Wang, R. et al. Engineering of covalent organic framework nanosheet membranes for fast and efficient ion sieving: charge-induced cation confined transport. *Small Methods* **9**, 2401111 (2025).
82. Peng, Y. et al. Mechanoassisted synthesis of sulfonated covalent organic frameworks with high intrinsic proton conductivity. *ACS Appl. Mater. Interfaces* **8**, 18505–18512 (2016).
83. Wu, Z. H. et al. Spatial size manipulation of 1D/2D channels in covalent organic framework membranes through dopamine chemistry for ion separations. *Adv. Funct. Mater.* **35**, 2416228 (2025).
84. Zhao, Z. et al. Horizontally arranged zinc platelet electrodeposits modulated by fluorinated covalent organic framework film for high-rate and durable aqueous zinc ion batteries. *Nat. Commun.* **12**, 6606 (2021).
85. Ren, L., Chen, J., Han, J., Liang, J. & Wu, H. Biomimetic construction of smart nanochannels in covalent organic framework membranes for efficient ion separation. *Chem. Eng. J.* **482** (2024). Ren et al. developed azobenzene-functionalized COF-Azo membranes via a biomimetic nanochannel modulation (BNM) strategy, forming charged and photo-switchable sub-nanochannels.
86. Yang, H. et al. Covalent organic framework membranes through a mixed-dimensional assembly for molecular separations. *Nat. Commun.* **10**, 2101 (2019).
87. Wang, J., Zhang, X., Shen, R., Yuan, Q. & Yang, Y. Staggered-stacking two-dimensional covalent organic framework membranes for molecular and ionic sieving. *ACS Nano* **18**, 34698–34707 (2024).
88. El-Kaderi, H. M. et al. Designed synthesis of 3D covalent organic frameworks. *Science* **316**, 268–272 (2007).
89. Berlanga, I. et al. Delamination of layered covalent organic frameworks. *Small* **7**, 1207–1211 (2011).

90. Bunck, D. N. & Dichtel, W. R. Bulk synthesis of exfoliated two-dimensional polymers using hydrazone-linked covalent organic frameworks. *J. Am. Chem. Soc.* **135**, 14952–14955 (2013).
91. Ying, Y. et al. A GO-assisted method for the preparation of ultrathin covalent organic framework membranes for gas separation. *J. Mater. Chem. A* **4**, 13444–13449 (2016).
92. Berlanga, I., Mas-Ballesté, R. & Zamora, F. Tuning delamination of layered covalent organic frameworks through structural design. *Chem. Commun.* **48**. <https://doi.org/10.1039/c2cc32187d> (2012).
93. Biswal, B. P., Chaudhari, H. D., Banerjee, R. & Kharul, U. K. Chemically stable covalent organic framework (COF)-polybenzimidazole hybrid membranes: enhanced gas separation through pore modulation. *Chem. Eur. J.* **22**, 4695–4699 (2016).
94. Kandambeth, S. et al. Selective molecular sieving in self-standing porous covalent-organic-framework membranes. *Adv. Mater.* **29**, 1603945 (2017). Banerjee et al. further developed a simple “casting dough” method as an alternative to prepare freestanding COF membranes.
95. Wang, L. et al. A highly soluble, crystalline covalent organic framework compatible with device implementation. *Chem. Sci.* **10**, 1023–1028 (2019).
96. Wang, R. et al. Ultrathin covalent organic framework membranes prepared by rapid electrophoretic deposition. *Adv. Mater.* **34**, 2204894 (2022).
97. Hao, S., Zhang, T., Fan, S., Jia, Z. & Yang, Y. Preparation of COF-TpPa1 membranes by chemical vapor deposition method for separation of dyes. *Chem. Eng. J.* **421**, 129750 (2021).
98. Shinde, D. B. et al. Crystalline 2D covalent organic framework membranes for high-flux organic solvent nanofiltration. *J. Am. Chem. Soc.* **140**, 14342–14349 (2018).
99. Martín-Illán, J. Á et al. Ultralarge free-standing imine-based covalent organic framework membranes fabricated *via* compression. *Adv. Sci.* **9**, 2104643 (2022).
100. Khan, N. A. et al. Assembling covalent organic framework membranes *via* phase switching for ultrafast molecular transport. *Nat. Commun.* **13**, 3169 (2022).
101. Yang, S.-T., Kim, J., Cho, H.-Y., Kim, S. & Ahn, W.-S. Facile synthesis of covalent organic frameworks COF-1 and COF-5 by sonochemical method. *RSC Adv.* **2**, 10179–10181 (2012).
102. Hao, D. et al. Fabrication of a COF-5 membrane on a functionalized α -Al₂O₃ ceramic support using a microwave irradiation method. *Chem. Commun.* **50**, 1462–1464 (2014).
103. Fu, J. et al. Fabrication of COF-MOF composite membranes and their highly selective separation of H₂/CO₂. *J. Am. Chem. Soc.* **138**, 7673–7680 (2016).
104. Fan, H., Gu, J., Meng, H., Knebel, A. & Caro, J. High-flux membranes based on the covalent organic framework COF-LZU1 for selective dye separation by nanofiltration. *Angew. Chem. Int. Ed.* **57**, 4083–4087 (2018).
105. Wu, T. et al. Imine-linked 3D covalent organic framework membrane featuring highly charged sub-1 nm channels for exceptional lithium-ion sieving. *Adv. Mater.* **37**, 2415509 (2025).
106. Ying, Y. et al. Ultrathin two-dimensional membranes assembled by ionic covalent organic nanosheets with reduced apertures for gas separation. *J. Am. Chem. Soc.* **142**, 4472–4480 (2020).
107. Li, G., Zhang, K. & Tsuru, T. Two-dimensional covalent organic framework (COF) membranes fabricated *via* the assembly of exfoliated COF nanosheets. *ACS Appl. Mater. Interfaces* **9**, 8433–8436 (2017).
108. Guo, Z. et al. Oil-water-oil triphase synthesis of ionic covalent organic framework nanosheets. *Angew. Chem. Int. Ed.* **60**, 27078–27085 (2021).
109. Wang, M. et al. Ultrafast seawater desalination with covalent organic framework membranes. *Nat. Sustain.* **5**, 518–526 (2022).
110. Valentino, L., Matsumoto, M., Dichtel, W. R. & Mariñas, B. J. Development and performance characterization of a polyimine covalent organic framework thin-film composite nanofiltration membrane. *Environ. Sci. Technol.* **51**, 14352–14359 (2017).
111. Matsumoto, M. et al. Lewis-acid-catalyzed interfacial polymerization of covalent organic framework films. *Chem* **4**, 308–317 (2018).
112. Wang, H. et al. Aqueous two-phase interfacial assembly of COF membranes for water desalination. *Nano Micro Lett.* **14**, 216 (2022).
113. Khan, N. A. et al. Solid-vapor interface engineered covalent organic framework membranes for molecular separation. *J. Am. Chem. Soc.* **142**, 13450–13458 (2020).
114. Zhang, Z. et al. Vapor-liquid interfacial polymerization of covalent organic framework membranes for efficient alcohol dehydration. *J. Membr. Sci.* **641**, 119905 (2022).
115. Zhao, S. et al. Hydrophilicity gradient in covalent organic frameworks for membrane distillation. *Nat. Mater.* **20**, 1551–1558 (2021).
116. Sahabudeen, H. et al. Highly crystalline and semiconducting imine-based two-dimensional polymers enabled by interfacial synthesis. *Angew. Chem. Int. Ed.* **132**, 6084–6092 (2020).
117. Yang, Y. et al. Elastic films of single-crystal two-dimensional covalent organic frameworks. *Nature* **630**, 878–883 (2024). Yang et al. utilized polyacrylic acid as a template and diethylenetriamine as a sacrificial go-between to direct the growth and crystallization of COF membranes, producing highly strong, tough, and elastic single-crystal 2D COF membranes.
118. Halder, A. et al. Ultrastable imine-based covalent organic frameworks for sulfuric acid recovery: an effect of interlayer hydrogen bonding. *Angew. Chem. Int. Ed.* **57**, 5797–5802 (2018).
119. Sasmal, H. S. et al. Superprotonic conductivity in flexible porous covalent organic framework membranes. *Angew. Chem. Int. Ed.* **130**, 11060–11064 (2018).
120. Halder, A. et al. Interlayer hydrogen-bonded covalent organic frameworks as high-performance supercapacitors. *J. Am. Chem. Soc.* **140**, 10941–10945 (2018).
121. Chen, L.-Y. et al. Interfacial synthesized covalent organic framework nanofiltration membranes for precisely ultrafast sieving. *Chem. Eng. J.* **430**, 133024 (2022).
122. Du, J. et al. Asymmetric ionic covalent organic framework membranes with tunable Turing patterns prepared *via* ion regulated strategy. *Nat. Commun.* **16**, 8664 (2025).
123. Hou, S. et al. Free-standing covalent organic framework membrane for high-efficiency salinity gradient energy conversion. *Angew. Chem. Int. Ed.* **60**, 9925–9930 (2021).
124. Cusin, L. et al. Synthesis of micrometre-thick oriented 2D covalent organic framework films by a kinetic polymerization pathway. *Nat. Synth.* **4**, 632–641 (2025). Cusin et al. utilized the casting method, combined with solvent evaporation and annealing processes, achieving the fabrication of a micrometre-thick oriented 2D COF membranes by leveraging a kinetically trapped amorphous 3D covalent adaptable network (CAN) intermediate.
125. Chen, S. et al. Imparting ion selectivity to covalent organic framework membranes using *de novo* assembly for blue energy harvesting. *J. Am. Chem. Soc.* **143**, 9415–9422 (2021).
126. Zuo, X. et al. Thermo-osmotic energy conversion enabled by covalent-organic-framework membranes with record output power density. *Angew. Chem. Int. Ed.* **61**, e202116910 (2022).
127. Cao, L. et al. Weakly humidity-dependent proton-conducting COF membranes. *Adv. Mater.* **32**, 2005565 (2020).
128. Zhu, T. et al. 3D covalent organic framework membrane with fast and selective ion transport. *Nat. Commun.* **14**, 5926 (2023).
129. Cao, L. et al. Giant osmotic energy conversion through vertical-aligned ion-permselective nanochannels in covalent organic framework membranes. *J. Am. Chem. Soc.* **144**, 12400–12409 (2022). Cao et al. developed two oriented COF membranes COF-SO₃H-x and COF-QA-x with cation and anion selectivity, respectively, *via* post-functionalization.

130. Wang, X. et al. Assembling covalent organic framework membranes with superior ion exchange capacity. *Nat. Commun.* **13**, 1020 (2022).
131. Lai, Z. et al. Covalent–organic–framework membrane with aligned dipole moieties for biomimetic regulable ion transport. *Adv. Funct. Mater.* **34**, 2409356 (2024).
132. Yin, S. et al. Giant gateable thermoelectric conversion by tuning the ion linkage interactions in covalent organic framework membranes. *Nat. Commun.* **15**, 8137 (2024).
133. Shi, X. et al. Flexible and robust three-dimensional covalent organic framework membranes for precise separations under extreme conditions. *Nano Lett.* **21**, 8355–8362 (2021).
134. Meng, Q.-W. et al. Optimizing selectivity via membrane molecular packing manipulation for simultaneous cation and anion screening. *Sci. Adv.* **10**, eado8658 (2024).
135. Afzal et al. Highly proton-conductive and stable sulfonated covalent organic framework hybrid membrane for vanadium redox flow battery. *J. Membr. Sci.* **722** <https://doi.org/10.1016/j.memsci.2025.123863> (2025).
136. Wang, A. et al. Selective ion transport through hydrated micropores in polymer membranes. *Nature* **635**, 353–358 (2024).
137. Wang, H. et al. Covalent organic framework membranes for efficient separation of monovalent cations. *Nat. Commun.* **13**, 7123 (2022). Wang et al. engineered negatively charged COF membranes via LBL assembly and demonstrated the precise separation for mono-/monovalent cations.
138. Niu, B. et al. Covalent organic frameworks embedded in polystyrene membranes for ion sieving. *Chem. Commun.* **58**, 5403–5406 (2022).
139. Bing, S. et al. Bio-inspired construction of ion conductive pathway in covalent organic framework membranes for efficient lithium extraction. *Matter* **4**, 1–12 (2021).
140. Liu, X., Lin, W., Al Mohawes, K. B. & Khashab, N. M. Guanidinium-based covalent organic framework membranes for superior mono- and divalent cations separation. *Small Struct.* **6**, 2400496 (2024).
141. Wang, M. et al. Construction of local-ion trap in phase-reversed mixed matrix COF membranes for ultrahigh ion selectivity. *Angew. Chem. Int. Ed.* e202504990 (2025).
142. Chu, X. et al. Optimization of cation selectivity based on channel chemistry of covalent organic framework under confined size. *J. Membr. Sci.* **722** <https://doi.org/10.1016/j.memsci.2025.123860> (2025).
143. Ren, X.-R. et al. Constructing stable chromenoquinoline-based covalent organic frameworks via intramolecular Povarov reaction. *J. Am. Chem. Soc.* **144**, 2488–2494 (2022).
144. Yang, C., Fu, X., Hou, L. & Hou, L. A. Gradient charge design of cationic covalent organic framework membranes toward enhanced acid recovery efficiency. *J. Membr. Sci.* **717** <https://doi.org/10.1016/j.memsci.2024.123606> (2025).
145. Yu, H. et al. Large-area soluble covalent organic framework oligomer coating for organic solution nanofiltration membranes. *Small* **20**, 2305613 (2024).
146. Corry, B. & Thomas, M. Mechanism of ion permeation and selectivity in a voltage-gated sodium channel. *J. Am. Chem. Soc.* **134**, 1840–1846 (2012).

Acknowledgements

We acknowledge funding from the National Key R&D Program of China (2022YFB3808500), National Natural Science Foundation of China (22422812, 22278387, 22208334, 52021002). Special thanks to the support of National Synchrotron Radiation, University of Science and Technology of China.

Author contributions

T. Xu and F. Sheng conceptualized the concept. All authors, including F. Sheng, L. Ge, X. Li, and T. Xu discussed the outline of this review. T. Xu and F. Sheng wrote the original draft. X. Li and T. Xu contributed to critical editing and refinement. Final approval was obtained from all authors.

Competing interests

The authors declare no competing interests.

Additional information

Supplementary information The online version contains supplementary material available at <https://doi.org/10.1038/s43246-025-01045-1>.

Correspondence and requests for materials should be addressed to Xingya Li or Tongwen Xu.

Peer review information *Communications Materials* thanks Yahui Cai and the other, anonymous, reviewer(s) for their contribution to the peer review of this work. A peer review file is available.

Reprints and permissions information is available at <http://www.nature.com/reprints>

Publisher's note Springer Nature remains neutral with regard to jurisdictional claims in published maps and institutional affiliations.

Open Access This article is licensed under a Creative Commons Attribution-NonCommercial-NoDerivatives 4.0 International License, which permits any non-commercial use, sharing, distribution and reproduction in any medium or format, as long as you give appropriate credit to the original author(s) and the source, provide a link to the Creative Commons licence, and indicate if you modified the licensed material. You do not have permission under this licence to share adapted material derived from this article or parts of it. The images or other third party material in this article are included in the article's Creative Commons licence, unless indicated otherwise in a credit line to the material. If material is not included in the article's Creative Commons licence and your intended use is not permitted by statutory regulation or exceeds the permitted use, you will need to obtain permission directly from the copyright holder. To view a copy of this licence, visit <http://creativecommons.org/licenses/by-nc-nd/4.0/>.

© The Author(s) 2026